

Learning Optimized Risk Scores from Large-Scale Datasets

Berk Ustun

USTUNB@MIT.EDU

Cynthia Rudin

RUDIN@MIT.EDU

*Massachusetts Institute of Technology
Cambridge, 02139 MA, USA*

Abstract

Risk scores are simple classification models that let users quickly assess risk by adding, subtracting and multiplying a few small numbers. These models are used for high-stakes applications in healthcare and criminology, but are difficult to learn from data because they need to be risk-calibrated, use small integer coefficients, and obey operational constraints. In this paper, we present a new approach to learn optimized risk scores from data by solving a discrete optimization problem. We formulate the risk score problem as a mixed integer nonlinear program, and present a new cutting plane algorithm to efficiently recover the optimal solution while avoiding the stalling behavior that occurs when we use existing cutting plane algorithms on non-convex problems. We pair our cutting plane algorithm with specialized procedures to generate feasible solutions, narrow the optimality gap, and reduce data-related computation. The resulting approach can learn optimized risk scores in a way that scales linearly in the number of samples, provides a proof of optimality, and accommodates complex operational constraints. We illustrate the benefits of our approach through extensive numerical experiments

Keywords: risk assessment; linear classification; cutting plane algorithms; integer programming; discrete optimization; risk scores; scoring systems.

1. Introduction

Risk scores are simple linear classification models that let users assess risk by adding, subtracting, and multiplying a few small numbers. These models are widely used in medicine and criminology because they let users make quick predictions, without extensive training, and without the use of a computer or calculator. They need to be accurate, risk-calibrated, sparse, and use small integer coefficients. In practice, domain experts may also require risk scores to satisfy operational constraints related to sparsity (“the model should use at most 10 features”), feature composition (“if the model uses $age \geq 60$ then it should also use $age \geq 80$ ”), and prediction (“the model should predict that males have higher risk than females”) among others.

In spite of their widespread use in high-stakes applications, there has been little to no work that has focused on a principled machine learning approach to build risk scores. Models that are currently used are created ad hoc, either by a panel of experts (see e.g., the CHADS₂ score of Gage et al., 2001) or by means of heuristics (e.g. by rounding logistic regression coefficients after choosing the input variables manually, as recommended by U.S. Department of Justice, 2005). Such approaches may lead to poor accuracy and/or risk

calibration (see e.g., the poor performance of CHADS₂ in Letham et al. 2013). Even an approach that is based on modern penalized logistic regression methods is ill-suited to create risk scores as it has to be paired with a rounding procedure to yield models with small integer coefficients. The resulting process combines several layers of approximations, requires extensive parameter tuning, and provides no guarantee as to whether it can produce a feasible model, let alone one that is optimal. As we will show, for constrained problems, this approach may fail to fit models that are accurate, risk-calibrated, and/or sparse, leading users to question whether a suitable risk score exists to begin with.

Our goal in this paper is to propose a new approach to learn risk scores by solving a discrete optimization problem. To this end, we formulate a mixed integer nonlinear program (MINLP) where the objective minimizes the logistic loss (for accuracy and risk calibration) and penalizes the ℓ_0 -norm (for sparsity), and where the constraints restrict coefficients to a small set of integers. We refer to the risk score obtained by solving this problem as a *Risk-Calibrated Supersparse Linear Integer Model* (RiskSLIM). In contrast to existing approaches, our approach lets users train risk scores that obey complex operational constraints without the need for parameter tuning, by directly adding logical constraints into the MINLP formulation. More importantly, it can recover a globally optimal solution and provide a guarantee on the optimality on any feasible solution. After solving the MINLP, we either end up with a suitable risk score, or are able to state (with certainty) that the model class we chose was too restrictive.

In light of these practical advantages, a major part of our paper consists in finding an algorithm that can consistently recover the optimal solution to the risk score problem and produce a certificate of optimality. As we show, solving the risk score problem by means of an off-the-shelf MINLP solver fails to exploit the structure of the problem, and spends a disproportionate amount of time on data-related computation, ultimately producing low quality models. Accordingly, we aim to solve the risk score problem by means of a cutting plane algorithm, which recovers the optimal solution to the MINLP by iteratively linearizing the logistic loss function. Cutting plane algorithms have an impressive track record in solving large-scale supervised learning problems (see Teo et al., 2007, 2009; Franc and Sonnenburg, 2008; Joachims et al., 2009). These algorithms have the advantage in that they scale linearly with the number of samples, can readily be parallelized, and can provide users with fine-grained control over data-related computation (Teo et al., 2007).

Unfortunately, existing cutting plane algorithms were designed under the assumption that they could solve the linearized problem to optimality at each iteration. Although this is a reasonable assumption for convex optimization problems, it also leads cutting plane algorithms to stall on non-convex problems. We demonstrate this phenomenon, and propose a new cutting plane algorithm to overcome this issue that we refer to as the *lattice cutting plane algorithm*. The resulting approach no longer suffers from the stalling issue, and maintains many of the previous advantages of cutting plane algorithms for a difficult discrete optimization problem – allowing us to learn optimized risk scores in a way that scales linearly in the number of samples, provides a proof of optimality, and accommodates complex operational constraints.

CONTRIBUTIONS

The main contributions of this paper are as follows:

- We propose the first principled approach to create risk scores. Our approach has the advantage that it can fit models that satisfy multiple operational constraints, recover the optimal model under such constraints, and assess the optimality of any model.
- We present a cutting plane algorithm for discrete optimization problems that avoids the stalling behavior of cutting plane algorithms designed for convex problems. Our proposed algorithm maintains the key benefits of existing methods, in that it scales linearly in the number of samples, can be parallelized, and can provide users with full control over data-related computation.
- We introduce specialized procedures for the lattice cutting plane algorithm that: (i) improve the rate at which it produces a proof of optimality; (ii) generate high quality feasible solutions; and (iii) reduce data-related computation. Two of these procedures – sequential rounding and discrete coordinate descent – can be used as standalone techniques to produce risk scores (heuristically).
- We provide an experimental comparison between our approach and heuristic approaches on publicly available datasets. Our approach produced risk score models in a matter of minutes. Our results also illustrate some of the pitfalls of approaches that are still used in practice.
- We provide software to create optimized risk scores using Python and the CPLEX API.

STRUCTURE

The remainder of our paper is structured as follows. In Section 1.1, we discuss related work. In Section 2, we formally describe the risk score problem. In Section 3, we briefly review cutting plane algorithms, explain why they stall on non-convex problems, and present our proposed lattice cutting plane algorithm. In Sections 4 and 5, we outline new techniques to improve the performance of the lattice cutting plane algorithm. In Section 6, we present experimental results to benchmark our risk scores to those produced using heuristic methods in terms of accuracy and risk calibration. In the appendices, we include: proofs of the theorems (Appendix A); details on numerical experiments from Sections 3 – 5 (Appendix B);

1.1 Related Work

In what follows, we discuss related work in risk scores, machine learning, and optimization.

RISK SCORES

Starting with the work of Burgess 1928, simple risk scores have been deployed in numerous high-stakes applications. Examples in criminology include: the Criminal History Category (U.S. Sentencing Commission, 1987); the Ohio Risk Assessment System (Latessa et al., 2009); the Kentucky Pretrial Risk Assessment Instrument (Austin et al., 2010); and the Offense Gravity Score (Pennsylvania Commission on Sentencing, 2012). Examples in medicine

include: SAPS I, II and III (Le Gall et al., 1984, 1993; Moreno et al., 2005) and APACHE I, II and III (Knaus et al., 1981, 1985, 1991) to assess ICU mortality risk.

Risk scores with few terms and small integer coefficients are often preferred in such applications due their high level of interpretability and their ability to make predictions without a computer and a calculator. Duwe and Kim (2016), for example, write: “*It is commonplace... for fine-tuned regression coefficients to be replaced with a simple-point system... to promote the easy implementation, transparency, and interpretability of risk-assessment instruments.*” Ridgeway (2013) provides similar reasons to justify why the LAPD uses a simple risk score to identify recruits who will become officers: “*A decent transparent model that is actually used will outperform a sophisticated system that predicts better but sits on a shelf. If the researchers had created a model that predicted well but was more complicated, the LAPD likely would have ignored it, thus defeating the whole purpose.*” Interpretability is a crucial requirement for models used in high-stakes applications (Kodratoff, 1994), as evidenced by the recent European Union ruling on the “right to an explanation” for algorithmic decision-making tools (Goodman and Flaxman, 2016).

The lack of a principled methodology for creating risk scores is best evidenced by the breadth of methods that are currently used in practice (see e.g., Bobko et al., 2007). Existing tools are built using ad hoc approaches that mix and match heuristics for fitting, rounding and feature selection. These approaches include: (i) having a panels of expert build the model by hand and using data for validation purposes only (see e.g., Gage et al., 2001); (ii) creating a risk score by assigning a coefficient of ± 1 to any input variable that is strongly/weakly correlated with the outcome (called the “Burgess” method as it was first used by Burgess, 1928); (iii) rounding the coefficients from a logistic regression model (Goel et al., 2015) or a linear probability model (U.S. Department of Justice, 2005) – sometimes referred to as the “weighted Burgess” method. Risk scores built using ad hoc approaches can perform poorly compared to models fit using modern methods (see e.g., the poor performance of CHADS₂ in Letham et al. 2013, and of risk scores built using the Burgess method in Duwe and Kim 2016). In light of the lack of a principled methodology for creating risk scores, a minor contribution of our work is a formal approach to build and evaluate these tools with existing machine learning methods

MACHINE LEARNING

The RISKSLIM models in this paper have the same form as the SLIM models in Ustun and Rudin 2015, but differ in terms of how they are used and built. RISKSLIM models are designed for risk assessment, and are built by solving a mixed-integer nonlinear program (MINLP) that optimizes the logistic loss. In contrast, SLIM models are designed for decision-making, and are built by solving a mixed-integer program (MIP) that optimizes the 0–1 loss. Optimizing the 0–1 loss does not necessarily produce models that are risk-calibrated or have high AUC. Optimizing the 0–1 loss is also \mathcal{NP} -hard (Nguyen and Sanner, 2013), so training SLIM models does not scale well to problems with a large number of samples (as is the case for RISKSLIM).

The risk score problem that we consider resembles the one in Ertekin and Rudin (2015) in that it minimizes the logistic loss and ℓ_0 -norm and restricts coefficients to a discrete set. Ertekin and Rudin (2015) solve this problem approximately using a Bayesian approach,

which has the benefit in that it can yield a posterior distribution on the coefficients. Here, we use an optimization approach, which has the benefits that it can consistently identify the globally optimal solution, assess optimality, and accommodate operational constraints. In addition, we propose new techniques to generate feasible solutions and reduce data-related computation that may improve the approach of Ertekin and Rudin (2015).

Our proposed methodology can be used to solve a broad range of machine learning problems that minimize a convex risk function with non-convex penalties or a non-convex feasible regions. Some examples include ℓ_0 -regularized linear regression, or discrete linear classification problems that minimize the hinge loss over a small set of integers (see e.g., Chevaleyre et al., 2013; Carrizosa et al., 2016; Malioutov and Varshney, 2013).

OPTIMIZATION

We fit risk scores by solving a MINLP with three key elements: (i) convex loss function; (ii) non-convex regularization penalty; (iii) discrete and bounded feasible region. In Section 3.3, we argue that this MINLP needs to be solved with a specialized algorithm given that off-the-shelf MINLP solvers fail to exploit the structure the problem and produce models that perform well on small instances. We note that recent work in the optimization literature has focused on specialized methods to solve problems that deal with some – but not all – of the key elements of our problem. Recent work in convex integer programming (Park and Boyd, 2015a), for instance, may be adapted to handle problems with a convex loss function and an discrete feasible region, but cannot readily handle a non-convex regularization penalty. Similarly, Hübner and Schöbel (2014) provide sufficient conditions under which the integer minimizer of a nonlinear optimization problem can be obtained by rounding the fractional minimizer. However, these conditions do not hold for our problem as the objective function and feasible region are non-convex due to the ℓ_0 penalty and operational constraints.

We solve the risk score problem with a cutting plane (CP) algorithm. CP algorithms have been extensively studied in the optimization community (see e.g., Kelley, 1960), and successfully used to solve large-scale machine learning problems (Teo et al., 2007, 2009; Franc and Sonnenburg, 2008). Our proposed lattice CP algorithm makes use of callback functions in modern MIP solvers, which can dynamically add cutting planes within a branch-and-bound search (see e.g., Bai and Rubin, 2009; Naoum-Sawaya and Elhedhli, 2010, for a similar uses of callback functions in the optimization literature). Lattice CP differs from current CP algorithms in that it does not *stall* on non-convex problems (i.e., it does not eventually get stuck solving an IP to optimality at each iteration). As we explain in Section 3.1, many CP algorithms will stall on non-convex problems (see Boyd and Vandenberghe, 2004, for a comprehensive list), including algorithms that are not typically used in machine learning, such as the center of gravity algorithm (Levin, 1965) or the analytic center algorithm (Atkinson and Vaidya, 1995).

2. Problem Statement

Our goal is to build risk assessment tools such as those shown in Figure 1.

1.	<i>Congestive Heart Failure</i>	1 point
2.	<i>Hypertension</i>	1 point	+
3.	<i>Age ≥ 75</i>	1 point	+
4.	<i>Diabetes Mellitus</i>	1 point	+
5.	<i>Prior Stroke or Transient Ischemic Attack</i>	2 points	+
ADD POINTS FROM ROWS 1 – 5		SCORE	=

SCORE	RISK
0	1.9%
1	2.8%
2	4.0%
3	5.9%
4	8.5%
5	12.5%
6	18.2%

Figure 1: CHADS₂ risk score of Gage et al. (2001) for assessing stroke risk.

We formalize this problem as follows. We start with a dataset of N i.i.d. training examples $\{(\mathbf{x}_i, y_i)\}_{i=1}^N$ where $\mathbf{x}_i \in \mathcal{X} \subseteq \mathbb{R}^{d+1}$ denotes a vector of features $[1, x_{i,1}, \dots, x_{i,d}]^T$ and $y_i \in \mathcal{Y} = \{\pm 1\}$ denotes a class label. We consider a linear score function $s(\boldsymbol{\lambda}, \mathbf{x}) = \langle \boldsymbol{\lambda}, \mathbf{x} \rangle$ where $\boldsymbol{\lambda} \subseteq \mathbb{R}^{d+1}$ represents a vector of coefficients $[\lambda_0, \lambda_1, \dots, \lambda_d]^T$, and λ_0 represents an intercept. We estimate the *predicted risk* that example i belongs to the positive class through the logistic link function as

$$\Pr(y_i = +1 \mid \mathbf{x}_i) = \frac{1}{1 + \exp(-\langle \boldsymbol{\lambda}, \mathbf{x}_i \rangle)}.$$

In this setup, each coefficient λ_j represents the number of points for a particular feature. Given an example with features \mathbf{x}_i , users tally the points to obtain a total score $s_i := \langle \boldsymbol{\lambda}, \mathbf{x}_i \rangle$, and then use the total score s_i to obtain an estimate of predicted risk. Alternatively, users could also obtain a predicted label $\hat{y}_i \in \{\pm 1\}$ by comparing the predicted risk to a threshold risk (e.g., predict $\hat{y}_i = +1$ iff $\Pr(y_i = +1) > 0.5$).

In practice, the desirable characteristics of a risk score include all of the following:

- *High AUC*: AUC measures the ability of the model to rank cases in terms of their predicted risk. A model with high AUC assigns larger scores to examples with higher risk compared to examples with lower risk.
- *Risk Calibration*: A risk-calibrated model outputs predicted probabilities that matched observed probabilities. Risk calibration ensures high AUC, but the converse is not true.
- *Sparsity and Small Integer Coefficients*: linear models that use a few small integer coefficients let users make quick predictions, without a computer or a calculator. In light of research showing that humans are limited in handling multiple cognitive entities (7 ± 2 according to Miller, 1984) and in estimating the association between three or more variables (Jennings et al., 1982), models with small integer coefficients help users gauge the

influence of each input variable and understand how multiple input variables are combined to output an estimate of predicted risk (as per the definition of interpretability in Hastie et al., 2011).

RISK SCORE PROBLEM

In this paper, we learn the values of the coefficients from the data by solving the following mixed integer nonlinear program (MINLP), which we refer to as the *risk score problem* or RISKSLIMMINLP:

$$\begin{aligned} \min_{\boldsymbol{\lambda}} \quad & l(\boldsymbol{\lambda}) + C_0 \|\boldsymbol{\lambda}\|_0 \\ \text{s.t.} \quad & \boldsymbol{\lambda} \in \mathcal{L}. \end{aligned} \tag{1}$$

Here, the objective minimizes the *logistic loss* $l(\boldsymbol{\lambda}) := \frac{1}{N} \sum_{i=1}^N \log(1 + \exp(-\langle \boldsymbol{\lambda}, y_i \mathbf{x}_i \rangle))$ for AUC and risk calibration, and penalizes the ℓ_0 -norm $\|\boldsymbol{\lambda}\|_0 := \sum_{j=0}^d \mathbb{1}[\lambda_j \neq 0]$ for sparsity. The trade-off parameter C_0 controls the balance between these two objectives. The feasible region restricts coefficients to a small set of bounded integers such as $\mathcal{L} = \{-5, \dots, 5\}^{d+1}$, and may be further customized to include any of the operational constraints in Table 1.

Constraint Type	Example
Feature Selection	Choose between 5 to 10 total features
Group Sparsity	Include either <i>male</i> or <i>female</i> in the model but not both
Risk Stratification	Use at most 3 thresholds for age indicator variables: $\sum_{k=1}^{100} \mathbb{1}[age \leq k] \leq 3$
Logical Structure	If <i>male</i> is in model, then include <i>hypertension</i> or <i>bmi</i> ≥ 30 as a control
Probability	Predict $\Pr(y = +1 \mathbf{x}) \geq 0.90$ when <i>male</i> = TRUE and <i>hypertension</i> = TRUE

Table 1: Operational constraints that can be enforced on risk scores by including additional constraints in the feasible region of RISKSLIMMINLP.

NOTATION

We use the following notation. We denote the objective of RISKSLIMMINLP using the function $V(\boldsymbol{\lambda}) := l(\boldsymbol{\lambda}) + C_0 \|\boldsymbol{\lambda}\|_0$, and denote its optimal solution as $\boldsymbol{\lambda}^* \in \operatorname{argmin}_{\boldsymbol{\lambda} \in \mathcal{L}} V(\boldsymbol{\lambda})$. In what follows, we refer to lower and upper bounds on important quantities related to the objective value function at $\boldsymbol{\lambda}^*$, which we denote as: $V(\boldsymbol{\lambda}^*) \in [V^{\min}, V^{\max}]$, $l(\boldsymbol{\lambda}^*) \in [L^{\min}, L^{\max}]$, $\|\boldsymbol{\lambda}^*\|_0 \in [R^{\min}, R^{\max}]$.

Unless otherwise specified, we make the following assumptions for clarity of exposition: (i) the coefficient set contains the null vector, $\mathbf{0} \in \mathcal{L}$; (ii) the intercept is never penalized, which means that the more precise version of the objective function in (1) is $V(\boldsymbol{\lambda}) := l(\boldsymbol{\lambda}) + C_0 \|\boldsymbol{\lambda}_{[1,d]}\|_0$ where $\boldsymbol{\lambda} = [\lambda_0, \boldsymbol{\lambda}_{[1,d]}]$. Here, the first assumption is to ensure that a generic formulation of RISKSLIMMINLP is always feasible, and the second assumption ensure that the intercept term is not regularized.

3. Methodology

In this section, we introduce the cutting plane algorithm that we use to solve the risk score problem, RISKSLIMMINLP. We first briefly review a conventional cutting plane algorithm to motivate why we would want to use them to solve RISKSLIMMINLP, and explain why current algorithms stall on non-convex problems such as RISKSLIMMINLP (Section 3.1). Next, we present a cutting plane algorithm that avoids the stalling behavior, which we refer to as the *lattice* cutting plane algorithm (Section 3.2). To illustrate the properties of different cutting plane algorithms and show that MINLP solvers fare poorly on RISKSLIMMINLP, we end this section with a comparison where we use these approach to solve difficult instances of RISKSLIMMINLP (Section 3.3).

3.1 Cutting Plane Algorithms

We show a conventional cutting plane algorithm that can be used to solve RISKSLIMMINLP in Algorithm 1.

Algorithm 1 recovers the optimal solution to RISKSLIMMINLP by iteratively solving a mixed-integer program (MIP) where the original loss function $l(\boldsymbol{\lambda})$ has been replaced with a piecewise linear approximation $\hat{l}^k(\boldsymbol{\lambda})$ built using k cutting planes. A *cutting plane* or *cut* to the loss function is a supporting hyperplane at a fixed point $\boldsymbol{\lambda}^k \in \mathcal{L}$ with the form

$$\theta \geq l(\boldsymbol{\lambda}^k) + \langle \nabla l(\boldsymbol{\lambda}^k), \boldsymbol{\lambda} - \boldsymbol{\lambda}^k \rangle.$$

Here, $\theta \in \mathbb{R}_+$ is an auxiliary variable that represents the value of the approximate loss function, and $l(\boldsymbol{\lambda}^k) \in \mathbb{R}_+$ and $\nabla l(\boldsymbol{\lambda}^k) \in \mathbb{R}^d$ are parameters that represent the value and gradient of the loss function at the point $\boldsymbol{\lambda}^k$

$$\begin{aligned} l(\boldsymbol{\lambda}^k) &= \frac{1}{N} \sum_{i=1}^N \log(1 + \exp(-\langle \boldsymbol{\lambda}^k, y_i \mathbf{x}_i \rangle)) \\ \nabla l(\boldsymbol{\lambda}^k) &= \frac{1}{N} \sum_{i=1}^N \frac{-y_i \mathbf{x}_i}{1 + \exp(-\langle \boldsymbol{\lambda}^k, y_i \mathbf{x}_i \rangle)}. \end{aligned} \tag{3}$$

Multiple cuts can be combined to build a piecewise linear approximation of the loss function as shown in Figure 2. If we denote a collection of k cuts at the points $\boldsymbol{\lambda}^1, \dots, \boldsymbol{\lambda}^k$ as

$$\mathcal{H}^k(\theta, \boldsymbol{\lambda}) = \bigcup_{t=1}^k \{\theta \geq l(\boldsymbol{\lambda}^t) + \langle \nabla l(\boldsymbol{\lambda}^t), \boldsymbol{\lambda} - \boldsymbol{\lambda}^t \rangle\},$$

then this cutting plane approximation of the loss function can be expressed as

$$\begin{aligned} \hat{l}^k(\boldsymbol{\lambda}) &= \min_{\theta \in \mathbb{R}} \mathcal{H}^k(\theta, \boldsymbol{\lambda}) \\ &= \min_{\substack{\theta \in \mathbb{R} \\ t=1, \dots, k}} \theta \geq l(\boldsymbol{\lambda}^t) + \langle \nabla l(\boldsymbol{\lambda}^t), \boldsymbol{\lambda} - \boldsymbol{\lambda}^t \rangle. \end{aligned}$$

On iteration k , Algorithm 1 solves a version of RISKSLIMMINLP that minimizes the cutting plane approximation $\hat{l}^k(\boldsymbol{\lambda})$ instead of the true loss function $l(\boldsymbol{\lambda})$. We refer to this

Algorithm 1 Cutting Plane Algorithm

Input

$(\mathbf{x}_i, y_i)_{i=1}^N$	training data
\mathcal{L}	RISKSLIMMINLP constraints
C_0	RISKSLIMMINLP ℓ_0 penalty parameter
$\varepsilon \leq 0$	tolerance in relative optimality gap

Initialize

$k \leftarrow 0$	iteration counter
$V^{\min} \leftarrow 0$	lower bound to the optimal value of RISKSLIMMINLP
$V^{\max} \leftarrow \infty$	upper bound to the optimal value of RISKSLIMMINLP
$\mathcal{H}^0(\theta, \boldsymbol{\lambda}) \leftarrow \{\theta \geq 0\}$	collection of cuts to the loss function

```

1 while  $\frac{V^{\max} - V^{\min}}{V^{\max}} > \varepsilon$  do
2   solve RISKSLIMMIP ( $\mathcal{H}^k(\theta, \boldsymbol{\lambda})$ ) to optimality and store optimizers  $\theta^k$  and  $\boldsymbol{\lambda}^k$ 
3   compute cut parameters  $l(\boldsymbol{\lambda}^k)$  and  $\nabla l(\boldsymbol{\lambda}^k)$ 
4    $\mathcal{H}^{k+1}(\theta, \boldsymbol{\lambda}) \leftarrow \mathcal{H}^k(\theta, \boldsymbol{\lambda}) \cup \{\theta \geq l(\boldsymbol{\lambda}^k) + \langle \nabla l(\boldsymbol{\lambda}^k), \boldsymbol{\lambda} - \boldsymbol{\lambda}^k \rangle\}$  ▷ add cut
5    $V^{\min} \leftarrow \theta^k + C_0 \|\boldsymbol{\lambda}^k\|_0$  ▷ lower bound is optimal value of RISKSLIMMIP ( $\mathcal{H}^k(\theta, \boldsymbol{\lambda})$ )
6    $V^k \leftarrow l(\boldsymbol{\lambda}^k) + C_0 \|\boldsymbol{\lambda}^k\|_0$ 
7   if  $V^k < V^{\max}$  then
8      $V^{\max} \leftarrow V^k$  ▷ update upper bound
9      $\boldsymbol{\lambda}^{\text{best}} \leftarrow \boldsymbol{\lambda}^k$  ▷ update best solution
10  end if
11   $k \leftarrow k + 1$ 
12 end while
    
```

Output: $\boldsymbol{\lambda}^{\text{best}}$, ε -optimal solution to RISKSLIMMINLP.

RISKSLIMMIP ($\mathcal{H}^k(\theta, \boldsymbol{\lambda})$) is a mixed integer program where the objective uses an approximate loss function built with the collection of cutting planes $\mathcal{H}^k(\theta, \boldsymbol{\lambda})$:

$$\begin{aligned}
 \min_{\theta, \boldsymbol{\lambda}} \quad & \theta + C_0 \|\boldsymbol{\lambda}\|_0 \\
 \text{s.t.} \quad & \theta \in \mathcal{H}^k(\theta, \boldsymbol{\lambda}), \\
 & \boldsymbol{\lambda} \in \mathcal{L}.
 \end{aligned} \tag{2}$$

The points $\theta^k, \boldsymbol{\lambda}^k$ are the optimizers of RISKSLIMMIP ($\mathcal{H}^k(\theta, \boldsymbol{\lambda})$).

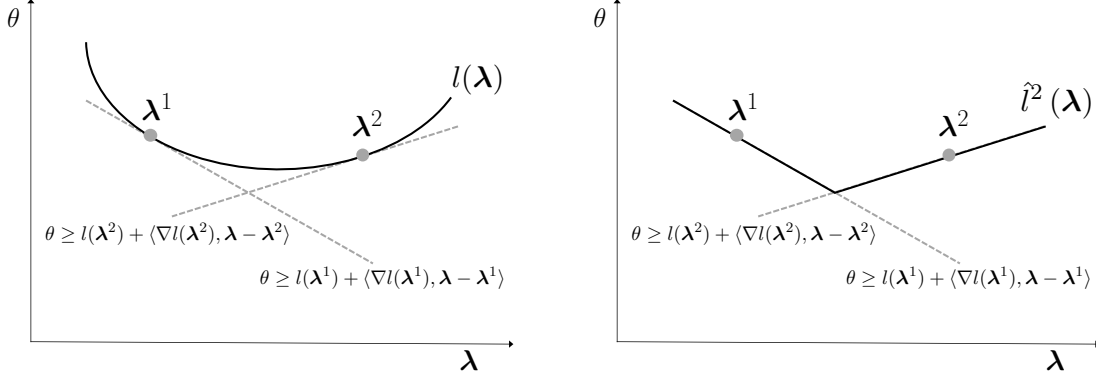


Figure 2: Cutting plane algorithms build a piecewise linear approximation of the loss function using a collection of cutting planes. The plot on the left shows the loss function $l(\boldsymbol{\lambda})$ with cutting planes at the points $\boldsymbol{\lambda}^1$ and $\boldsymbol{\lambda}^2$. The plot on the right shows the approximate loss function $\hat{l}^2(\boldsymbol{\lambda}) = \min_{\theta} \mathcal{H}^2(\theta, \boldsymbol{\lambda})$ where $\mathcal{H}^2(\theta, \boldsymbol{\lambda})$ is the collection of cutting planes $\bigcup_{t=1}^2 \{\theta \geq l(\boldsymbol{\lambda}^t) + \langle \nabla l(\boldsymbol{\lambda}^t), \boldsymbol{\lambda} - \boldsymbol{\lambda}^t \rangle\}$. As shown, for a convex loss function, $\hat{l}^k(\boldsymbol{\lambda}) \leq l(\boldsymbol{\lambda})$ for all $k \in \mathbb{N}$ and $\boldsymbol{\lambda} \in \mathcal{L}$.

surrogate problem as RISKSLIMMIP ($\mathcal{H}^k(\theta, \boldsymbol{\lambda})$) and denote its optimal solution as $(\theta^k, \boldsymbol{\lambda}^k)$. The solution $(\theta^k, \boldsymbol{\lambda}^k)$ from each iteration is used in two distinct ways: (i) to construct a new cutting plane that will improve the approximate loss function; and (ii) to update the upper bound and lower bound on the optimal value of RISKSLIMMINLP and assess convergence. Here, the upper bound V^{\max} is produced using the best solution across all iterations

$$V^{\max} = \min_{t=1, \dots, k} V(\boldsymbol{\lambda}^t).$$

The lower bound is produced by using the optimal solution at each iteration $(\theta^k, \boldsymbol{\lambda}^k)$ as

$$V^{\min} = \theta^k + C_0 \|\boldsymbol{\lambda}^k\|_0.$$

To see how this quantity constitutes a lower bound, note that a convex function is always underestimated by its cutting plane approximation, so that $\hat{l}^k(\boldsymbol{\lambda}) \leq l(\boldsymbol{\lambda})$ for all $k \in \mathbb{N}$ and $\boldsymbol{\lambda} \in \mathcal{L}$ (see Figure 2). In particular, for $\boldsymbol{\lambda}^* \in \operatorname{argmin}_{\boldsymbol{\lambda} \in \mathcal{L}} V(\boldsymbol{\lambda})$, we have

$$\hat{l}^k(\boldsymbol{\lambda}^*) + C_0 \|\boldsymbol{\lambda}^*\|_0 \leq l(\boldsymbol{\lambda}^*) + C_0 \|\boldsymbol{\lambda}^*\|_0 = V(\boldsymbol{\lambda}^*)$$

Since Algorithm 1 picks $\boldsymbol{\lambda}^k$ as the minimizer of $\hat{l}^k(\boldsymbol{\lambda}) + C_0 \|\boldsymbol{\lambda}\|_0$, it follows that

$$\theta^k + C_0 \|\boldsymbol{\lambda}^k\|_0 = \hat{l}^k(\boldsymbol{\lambda}^k) + C_0 \|\boldsymbol{\lambda}^k\|_0 \leq \hat{l}^k(\boldsymbol{\lambda}^*) + C_0 \|\boldsymbol{\lambda}^*\|_0 \leq V(\boldsymbol{\lambda}^*)$$

Algorithm 1 converges to ε -optimal solution of RISKSLIMMINLP in a fixed number of iterations (see Kelley, 1960, for a proof). To see this, note that the cutting plane approximation of a convex loss function improves monotonically with each additional cut:

$$\hat{l}^k(\boldsymbol{\lambda}) \leq \hat{l}^{k+m}(\boldsymbol{\lambda}) \leq l(\boldsymbol{\lambda}) \text{ for all } k, m \in \mathbb{N} \text{ and } \boldsymbol{\lambda} \in \mathcal{L}. \quad (4)$$

Since the cuts added in Step 4 of Algorithm 1 at each iteration are not redundant, the lower bound V^{\min} improves monotonically with each iteration. Eventually, the relative optimality gap, $\frac{V^{\max} - V^{\min}}{V^{\max}}$ is less than a user-specified tolerance ε . At this point, the best solution $\boldsymbol{\lambda}^{\text{best}}$ found by the cutting-plane algorithm provably belongs to the ε -level set of solutions to RISKSLIMMINLP.

BENEFITS OF SOLVING RISKSLIMMINLP WITH A CUTTING PLANE ALGORITHM

A cutting plane algorithm is well-suited for solving RISKSLIMMINLP since it eliminates the nonlinearity in the objective by replacing the loss function with a piecewise linear approximation. This lets us build risk scores by iteratively solving RISKSLIMMIP ($\mathcal{H}^k(\theta, \boldsymbol{\lambda})$), meaning that we can use a MIP solver instead of a MINLP solver. MIP solvers exhibit far better off-the-shelf performance than MINLP solvers due to fact that MINLP solvers are designed to handle a diverse set of optimization problems. In other words, by using a cutting plane algorithm, we exploit the structure of the problem to get better performance. As we show in Section 3.3, the resulting performance improvement in using a cutting plane algorithm may be substantial, even as the cutting plane algorithm has to solve multiple MIPs while a MINLP solver only has to solve a single MINLP.

In addition, Algorithm 1 illustrates several key benefits of cutting plane algorithms for general risk minimization problems, namely scalability in the sample size and control over data-related computation (see also Teo et al., 2007; Franc and Sonnenburg, 2008). Specifically, cutting plane algorithms only use the training data to compute the cut parameters as in Step 3 of Algorithm 1. As shown in Figure 3, this guarantees scalability as cut parameters can be computed using elementary matrix-vector operations that scale at $O(Nd)$, meaning on a problem where d is fixed, running time scales linearly in N . In practice, cutting plane algorithms also provide a useful degree flexibility in that we can compute cut parameters use a customized implementation that, for example, makes use of distributed computation, does not require the data to be stored locally, and/or reduces data-related computation by exploiting properties of the model class (see Section 5 for an example).

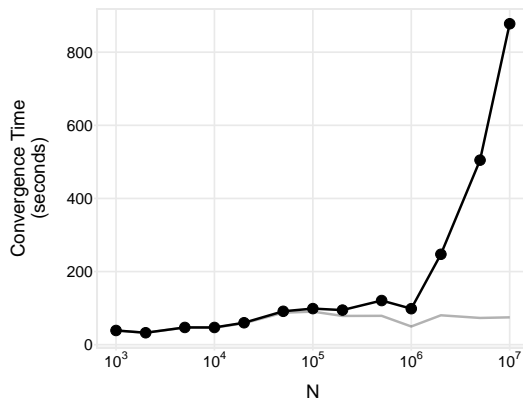


Figure 3: Convergence time of Algorithm 1 on simulated datasets with $d = 10$ dimensions at varying sample sizes N . The grey line corresponds to the runtime for the MIP solver, which excludes the time to compute cuts. As N increases, solver time remains roughly constant and the time to compute cuts increases at $O(N)$. We include details on the data and setup for this experiment in Appendix B.

STALLING BEHAVIOR ON NON-CONVEX PROBLEMS

Algorithm 1 is similar to cutting-plane algorithms used for large-scale machine learning problems (see e.g., Teo et al., 2009; Franc and Sonnenburg, 2008) in that it solves an optimization problem at each iteration (see Step 5). When these algorithms are used to solve convex optimization problems, the surrogate problem that has to be solved at each iteration is also convex and therefore relatively easy to solve. However, when they are applied to non-convex problems, such as RISKSLIMINLP, the surrogate problem that has to be solved at each iteration, RISKSLIMMIP, is non-convex and may be intractable.

In practice, the need to solve a non-convex surrogate problem at each iteration leads cutting plane algorithms to *stall*, as the algorithm eventually encounters a non-convex surrogate optimization problem that requires a disproportionate amount of time to solve. We illustrate this stalling behavior of Algorithm 1 in Figure 4. As shown, the few iterations of Algorithm 1 can easily produce a certificate of optimality when RISKSLIMMIP $(\mathcal{H}^k(\theta, \lambda))$ contains a trivial approximation of the loss function. However, RISKSLIMMIP $(\mathcal{H}^k(\theta, \lambda))$ becomes increasingly difficult to optimize as a new cutting plane is added at each iteration, and the loss function is better approximated. On the $d = 10$ instance, the MIP solver is powerful enough to solve RISKSLIMMIP $(\mathcal{H}^k(\theta, \lambda))$ to optimality across all iterations. On the $d = 20$ instance, however, the time to find the optimal solution and prove optimality begins to increase exponentially, leading the Algorithm 1 to stall as the 86th iteration.

Note there is no easy fix to address the stalling of cutting plane algorithms such as Algorithm 1 on non-convex problems such as RISKSLIMINLP. The reason for this is because these algorithms require a provably optimal solution to a non-convex surrogate problem at each iteration to produce a valid lower bound and assess convergence. In the case of RISKSLIMINLP, this means that they must not only find the optimal solution to RISKSLIMMIP $(\mathcal{H}^k(\theta, \lambda))$ at each iteration, but also prove that this solution is opti-

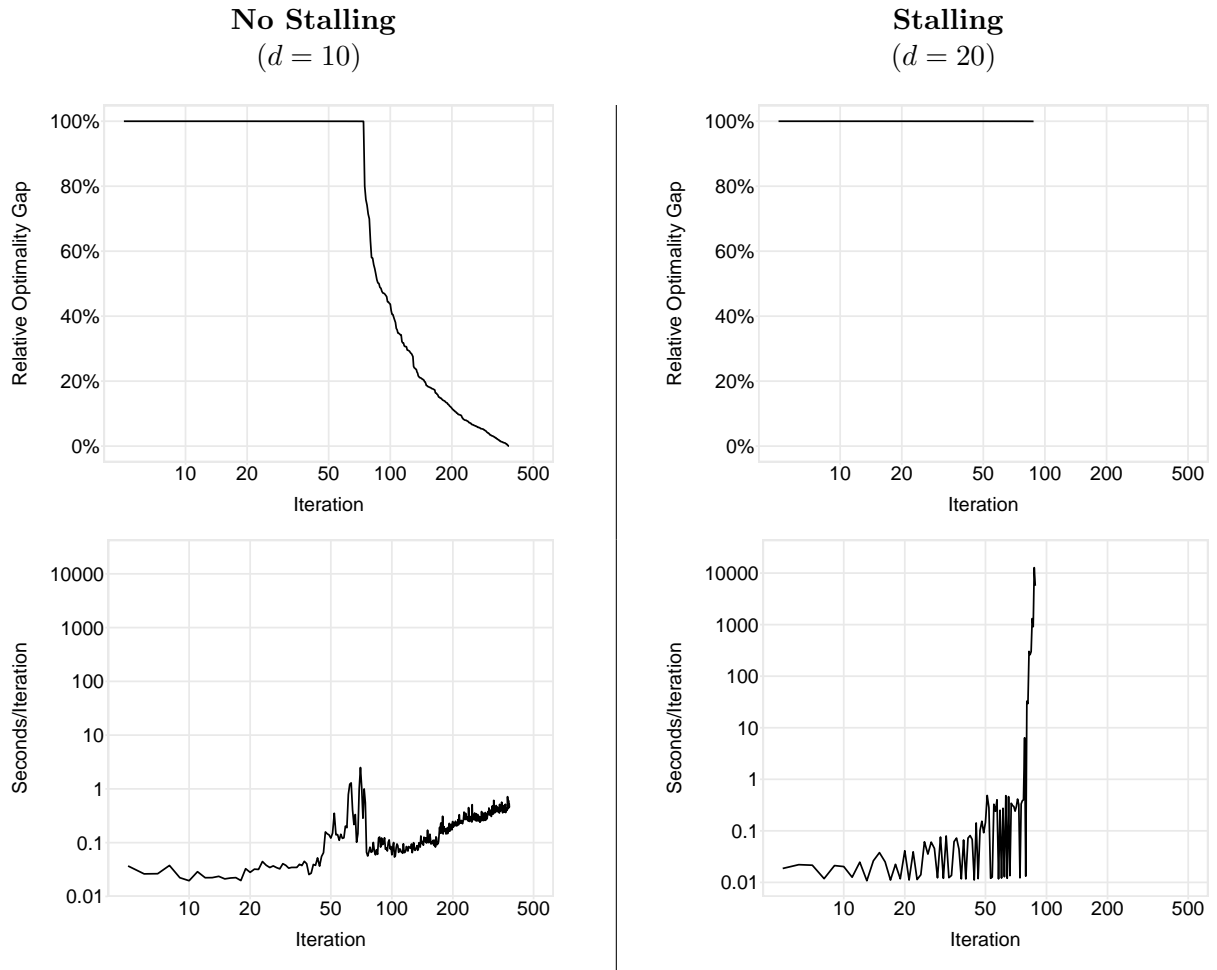


Figure 4: Performance of Algorithm 1 on simulated datasets with $N = 50\,000$ samples with $d = 10$ and $d = 20$ dimensions. We plot the relative optimality gap at each iteration (top), and the time per iteration in log-scale (bottom) below. As shown, the algorithm stalls on the $d = 20$ problem as the time to solve RISKSLIMMIP to optimality increases exponentially starting on iteration 86.

mal by returning a relative optimality gap of 0%. If, for example, we stopped solving RISKSLIMMIP ($\mathcal{H}^k(\theta, \lambda)$) at a feasible solution that we did not know was optimal, then the lower bound V^{\min} could exceed the true optimal value of RISKSLIMMINLP, in which case the algorithm would stop early and return a suboptimal solution with invalid bounds. Seeing how stalling is tied to the need to assess convergence, an alternative (but also flawed) approach is to solve RISKSLIMMINLP with a cutting plane algorithm that adds cuts at central points of RISKSLIMMIP ($\mathcal{H}^k(\theta, \lambda)$) (e.g., the center of gravity method of Levin 1965 or the analytic center methods of Atkinson and Vaidya 1995; Goffin and Vial 2002), as these methods can guarantee convergence in a fixed number of iterations through spatial arguments. In this case, however, stalling would still occur as we would have to solve a different non-convex optimization problem at each iteration to compute central points.

3.2 Lattice CPA

To fix the stalling behavior of the conventional CP algorithm, we present the lattice CP algorithm shown in Algorithm 2. Similar algorithms have been used in the optimization literature (see e.g., Bai and Rubin, 2009), but have not been applied to solve risk minimization problems as we do here.

The lattice CP algorithm 2 dynamically adds cutting planes as feasible solutions are uncovered in a single branch-and-bound tree. It provides a proof of optimality by computing upper and lower bounds. As in the conventional CP, the upper bound is computed using feasible solutions. The lower bound, however, is computed using the lowest value of the LP relaxation to RISKSLIMMIP (k) across all of the partitions in the branch-and-bound tree.

Once the lattice CP algorithm finds a feasible solution (termed the incumbent solution), it aims to prove that the solution is optimal using a branch-and-bound strategy (i.e. by showing that all solutions belong to partitions that are either infeasible, or that are guaranteed to attain a larger objective value). If in this process, it encounters a feasible solution that attains a better objective value, then it updates the incumbent solution.

Here, RISKSLIMLP ($\mathcal{H}(\theta, \lambda), \mathcal{R}$) is the linear programming (LP) relaxation of RISKSLIMMIP ($\mathcal{H}(\theta, \lambda)$) shown in (5). We parameterize RISKSLIMLP ($\mathcal{H}(\theta, \lambda), \mathcal{R}$) according \mathcal{R} because we will repeatedly solve this problem over different partitions.

The main differences between the conventional CP and lattice CP algorithms are that the lattice CP algorithm does not stall, and that the lattice CP algorithm produces a weaker lower bound at each iteration. Thus, for instances where the conventional CP does not get stuck, it may actually converge faster than the lattice CP because it produces a stronger lower bound at each iteration (see e.g., the performance profile in Figure 4 for $d = 10$).

We note that although the algorithm itself seems more complicated, the implementation is easy. CPLEX handles the branch and bound. The implementation is done using callback functions. One advantage of this is that modern solvers can implement cut constraints as lazy constraints – meaning that the constraints are typically only applied when they are needed. CPLEX, for instance, guarantees that all lazy constraints are satisfied before yielding any integer feasible solution. This makes CPLEX good at dealing with the huge number of lazy constraints that may be generated in the process.

Algorithm 2 Lattice Cutting Plane Algorithm

Input

$(\mathbf{x}_i, y_i)_{i=1}^N$	training data
\mathcal{L}	RISKSLIMMINLP constraints
C_0	RISKSLIMMINLP ℓ_0 penalty parameter
$\varepsilon \geq 0$	tolerance in relative optimality gap
NODESELECTIONRULE	provided by MIP solver
PARTITIONSPLITTINGRULE	provided by MIP solver

Initialize

$(V^{\min}, V^{\max}) \leftarrow (0, \infty)$	lower and upper bounds on the optimal value of RISKSLIMMINLP
$\mathcal{H}(\theta, \boldsymbol{\lambda}) \leftarrow \{\theta \geq 0\}$	collection of cutting planes to the loss function
$\mathcal{R}^0 \leftarrow \text{conv}(\mathcal{L})$	partition for the root node
$V^0 \leftarrow V^{\min}$	lower bound for the root node
$\text{NODESET} \leftarrow \{(\mathcal{R}^0, V^0)\}$	set of nodes to explore in the branch-and-bound tree

```

1 while  $\frac{V^{\max} - V^{\min}}{V^{\max}} > \varepsilon$  and  $\text{NODESET} \neq \emptyset$  do
2   pick and remove  $(\mathcal{R}^r, V^r)$  from  $\text{NODESET}$  using  $\text{NODESELECTIONRULE}$ 
3   solve RISKSLIMLP  $(\mathcal{H}^k(\theta, \boldsymbol{\lambda}), \mathcal{R}^r)$  to obtain optimizers  $(\theta^r, \boldsymbol{\lambda}^r)$  ▷ if infeasible, goto Step 2
4    $V \leftarrow \theta^r + C_0 \|\boldsymbol{\lambda}^r\|_0$ 
5   if  $\boldsymbol{\lambda}^r \in \mathcal{L}$  then
6     compute cutting plane parameters  $l(\boldsymbol{\lambda}^r)$  and  $\nabla l(\boldsymbol{\lambda}^r)$ 
7      $\mathcal{H}^{k+1}(\theta, \boldsymbol{\lambda}) \leftarrow \mathcal{H}^k(\theta, \boldsymbol{\lambda}) \cup \{\theta \geq l(\boldsymbol{\lambda}^r) + \langle \nabla l(\boldsymbol{\lambda}^r), \boldsymbol{\lambda} - \boldsymbol{\lambda}^r \rangle\}$  ▷ add cut
8     if  $V < V^{\max}$  then
9        $\boldsymbol{\lambda}^{\text{best}} \leftarrow \boldsymbol{\lambda}^r, V^{\max} \leftarrow V$  ▷ update incumbent
10      remove all nodes  $(\mathcal{R}^s, V^s) \in \text{NODESET}$  s.t.  $V^s \geq V^{\max}$ 
11    end if
12     $k \leftarrow k + 1$ 
13  else
14    split  $\mathcal{R}^r$  into  $\mathcal{R}^I$  and  $\mathcal{R}^{II}$  using  $\text{PARTITIONSPLITTINGRULE}$ 
15    add  $(\mathcal{R}^I, V)$  and  $(\mathcal{R}^{II}, V)$  to  $\text{NODESET}$ 
16     $V^{\min} \leftarrow \min(V, V^{\min})$ 
17  end if
18 end while
    
```

Output: $\boldsymbol{\lambda}^{\text{best}}$, ε -optimal solution to RISKSLIMMINLP

RISKSLIMLP $(\mathcal{H}(\theta, \boldsymbol{\lambda}), \mathcal{R})$ is a linear programming (LP) relaxation of RISKSLIMMIP $(\mathcal{H}(\theta, \boldsymbol{\lambda}))$ where $\boldsymbol{\lambda}$ belongs to the partition $\mathcal{R} \subseteq \text{conv}(\mathcal{L})$:

$$\begin{aligned}
 \min_{\theta, \boldsymbol{\lambda}, \boldsymbol{\alpha}} \quad & \theta + C_0 \sum_{j=1}^d \alpha_j \\
 \text{s.t.} \quad & \theta \in \mathcal{H}(\theta, \boldsymbol{\lambda}) \\
 & \boldsymbol{\lambda} \in \mathcal{R} \\
 & \alpha_j = \frac{\max(\lambda_j, 0)}{\Lambda_j^{\max}} + \frac{\min(\lambda_j, 0)}{\Lambda_j^{\min}} \text{ for } j = 1, \dots, d
 \end{aligned} \tag{5}$$

3.3 Empirical Performance of Algorithms to Solve RiskSLIMMINLP

To illustrate the real-world performance of both cutting plane algorithms, we used each algorithm to solve difficult instances of RISKSLIMMINLP on simulated datasets with varying dimensions d and sample sizes N (see Appendix B for details). As a baseline, we also solved these instances using a commercial MINLP solver (Artelsys Knitro 9.0, which is an updated version of the MINLP solver from Byrd et al., 2006)¹.

In Figure 15, we compare the performance of all three methods in terms of the following metrics:

- time to find a near-optimal solution without a proof of optimality (i.e., within 10% of the optimal solution, which typically results in near-optimal AUC and risk calibration)
- relative optimality gap at termination (i.e., 0% iff the method finds the optimal solution and provides a proof of optimality within the 6 hour time limit)
- time spent on data-related computation (i.e., time spent evaluating the value, gradient, or Hessian of the loss function)

As shown, the MINLP solver could only solve small instances of RISKSLIMMINLP that stem from datasets with few samples and/or dimensions. On larger instances, the solver not only fails to converge within the 6-hour time limit, but also fails to produce a high quality feasible solution. One reason for this is that the MINLP solver spend the majority of its time dealing with operations that involve data-related computation. Seeing how a MINLP solver is designed to solve a diverse set of optimization problems, it is unlikely that it will be able to identify and exploit the specific structure of the risk score problem in the same way as the cutting-plane algorithms. In fact, it may even attempt to solve RISKSLIMMINLP in a way that is particularly inefficient (e.g. by repeatedly estimating or evaluating the Hessian of the objective function)

1. There exist several off-the-shelf MINLP solvers (see Bussieck and Vigerske, 2010, for a list). We chose Knitro because it let us: (i) control / reduce data-related computation (by letting us write our own function handles for the objective, its gradient and Hessian); (ii) solve LP subproblems using CPLEX, which is the same solver that we used for our algorithms; (iii) solve RISKSLIMMINLP using different MINLP algorithms (we tested 3, which all behave similarly; we only show the best performing in Figure 15 and include results for the remaining MINLP algorithms in Appendix B).

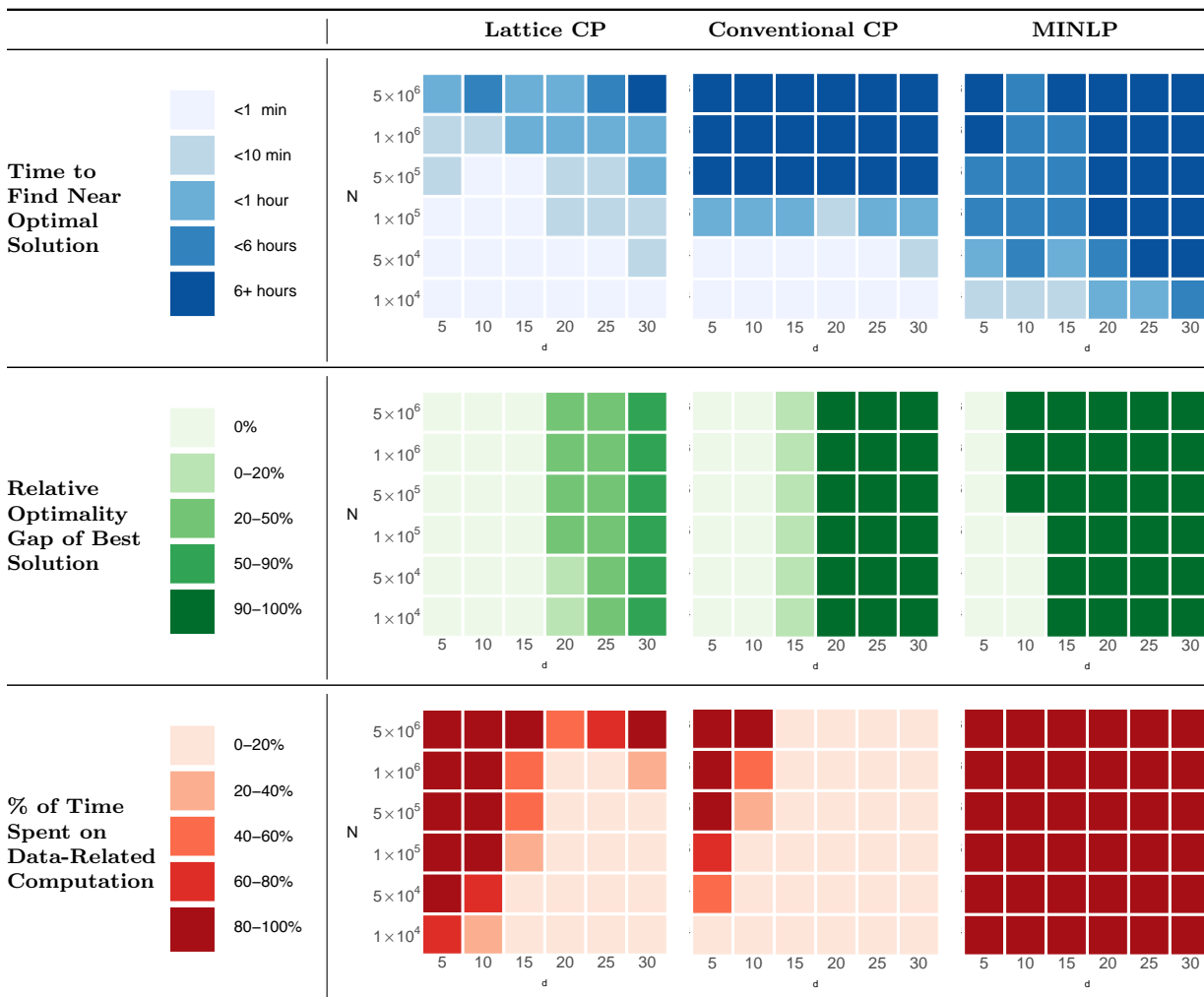


Figure 5: Comparison of algorithms to solve RISKSLIMMINLP on simulated datasets with varying dimensions d and sample sizes N . Lattice CP can find a high quality solution in less time than other approaches, especially on large datasets. Both Lattice CP and Conventional CP scale linearly in N (i.e., if these methods can solve an instance for fixed d , then they can solve instances with larger N at little additional cost). Conventional CP and MINLP cannot find high quality solution on datasets with larger dimensions as they either stall (conventional CP), or spend the majority of time dealing with data-related computation (MINLP). We include details on the data and setup for this experiment in Appendix B.

4. Algorithmic Improvements

In this section, we present several techniques to improve the performance of the lattice CP algorithm on the risk score problem.

4.1 Generating High Quality Feasible Solutions

In what follows, we present two procedures to generate and polish feasible solutions for the risk score problem, RISKSLIMMINLP. These procedures can be used in Algorithm 2 to generate new feasible solutions, improve existing feasible solutions, and narrow the optimality gap by reducing the upper bound. As we show in Section 6, these procedures can also be combined with a standard logistic regression method to build risk scores without solving RISKSLIMMINLP.

4.1.1 DISCRETE COORDINATE DESCENT

Discrete coordinate descent (DCD) is a heuristic procedure for polishing integer feasible solutions (Algorithm 3). It takes as input an integer feasible solution $\boldsymbol{\lambda} = (\lambda_0, \dots, \lambda_d) \in \mathcal{L}$ and iteratively shifts the value of one coordinate λ_j to produce a new integer feasible solution with a lower objective value. DCD is greedy in that the descent direction at each iteration is chosen as the dimension $j \in \{0, \dots, d\}$ that results in the largest decrease in the objective value of RISKSLIMMINLP $j \in \operatorname{argmin} V(\boldsymbol{\lambda} + \delta_j e_j)$. It does not cycle, terminates in a finite number of iterations, and outputs a polished integer feasible solution that is *1-opt* with respect to the objective value of RISKSLIMMINLP. That is, a solution such that the objective value does not improve in any single dimension².

The most expensive part of Algorithm 3 is the minimization in Step 4 in which we need to determine a step-size $\delta_j \in \Delta_j$ that minimizes the objective value in dimension j . The minimization can be implemented using a naive exhaustive search strategy that computes the loss at all valid step-sizes $\delta_j \in \Delta_j$. In our implementation, we use a bisection search algorithm that exploits the convexity of the loss function and reduces the number of loss function evaluations. This approach requires a total of $\log_2(|\mathcal{L}_j|)Nd$ flops per iteration, which is an improvement over the $(|\mathcal{L}_j| - 1)Nd$ flops per iteration required from the naive exhaustive search strategy (i.e., where we evaluate the loss for all $(|\mathcal{L}_j| - 1)$ values of λ_j other than current value).

DCD can be used as a subroutine in Algorithm 2 to improve the objective value of any feasible solution (e.g., when the solver finds a feasible solution in Step 7). If the procedure outputs a polished solution that is also feasible, then this may update the upper bound V^{\max} in Step 9, and thereby reduce the optimality gap. Alternatively, DCD can also be used to polish integer feasible solutions from the sequential rounding procedure in Section 4.1.2, and as part of the initialization procedure in Section 4.2.2.

2. 1-opt is a local optimality guarantee for discrete optimization problems (see e.g., Park and Boyd, 2015b, for a 1-opt heuristic on a different discrete optimization problem).

Algorithm 3 Discrete Coordinate Descent

Input

$(\mathbf{x}_i, y_i)_{i=1}^N$	training data
\mathcal{L}	RISKSLIMMINLP constraints
C_0	RISKSLIMMINLP ℓ_0 penalty parameter
$\boldsymbol{\lambda} \in \mathcal{L}$	feasible solution to RISKSLIMMINLP

Initialize

$V \leftarrow V(\boldsymbol{\lambda})$	objective value at current solution
$\mathcal{J} \leftarrow \{1, \dots, d\}$	valid search dimensions

```

1 repeat
2   for  $j \in \mathcal{J}$  do
3      $\Delta_j \leftarrow \{\delta \in \mathbb{Z} \mid \boldsymbol{\lambda} + \delta e_j \in \mathcal{L}\}$  ▷ list feasible moves along dim  $j$ 
4      $\delta_j \leftarrow \operatorname{argmin}_{\delta \in \Delta_j} V(\boldsymbol{\lambda} + \delta)$  ▷ find best move along dim  $j$ 
5      $v_j \leftarrow V(\boldsymbol{\lambda} + \delta_j e_j)$  ▷ store objective value for best move along dim  $j$ 
6   end for
7    $m \leftarrow \operatorname{argmin}_{j \in \mathcal{J}} v_j$  ▷ find descent dimension
8   if  $v_m < V$  then
9      $V \leftarrow v_m$ 
10     $\boldsymbol{\lambda} \leftarrow \boldsymbol{\lambda} + \delta_m e_m$ 
11     $\mathcal{J} \leftarrow \{1, \dots, d\} \setminus \{m\}$  ▷ ignore dim  $m$  on next iteration
12  end if
13 until  $v_m \geq V$ 

```

Output: $\boldsymbol{\lambda}$, set of coefficients that is 1-opt with respect to the objective of RISKSLIMMINLP

4.1.2 SEQUENTIAL ROUNDING

Sequential rounding (Algorithm 4) is a heuristic to generate an integer feasible solution $\lambda \in \mathcal{L}$ by rounding a continuous solution $\lambda^{\text{cts}} \in \text{conv}(\mathcal{L})$ in a way that accounts for the objective value of RISKSLIMMINLP.

Given a continuous solution λ^{cts} , sequential rounding returns one of its 2^d possible roundings in a d step procedure that rounds one component at a time, either upwards or downwards. On step k , the procedure has already rounded $k - 1$ components, and needs to round one of the $d - k - 1$ remaining continuous components λ_j^{cts} $j \in \mathcal{J}^{\text{cts}}$ either to $\lceil \lambda_j^{\text{cts}} \rceil$ or $\lfloor \lambda_j^{\text{cts}} \rfloor$. To do this, it evaluates the objective value of RISKSLIMMINLP at all possible roundings, and then chooses to round the component that minimizes the objective value of RISKSLIMMINLP. Thus, the k^{th} step requires a total of $\sum_{i=1}^{d-k} 2i = (d - k)(d - k + 1)$ evaluations of the loss function, and the entire procedure requires a total of $\frac{1}{3}d(d^2 - 1)$ evaluations of the loss function.

Sequential rounding can be paired with Algorithm 2 to produce integer feasible solutions using continuous solutions that are obtained from solving RISKSLIMLP in Step 3. If this outputs an integer feasible solution that improves upon the current best solution, then it will update the upper bound V^{max} in Step 9, and thereby improve the optimality gap. In our implementation, we pair sequential rounding with DCD from Section 4.1.1, and use it as part of the initialization procedure in Section 4.2.2.

Algorithm 4 Sequential Rounding

Input

$(\mathbf{x}_i, y_i)_{i=1}^N$	data
$\lambda \in \text{conv}(\mathcal{L})$	feasible solution to RISKSLIMLP
\mathcal{L}	RISKSLIMMINLP constraints
C_0	RISKSLIMMINLP ℓ_0 penalty parameter

Initialize

$\mathcal{J}^{\text{cts}} \leftarrow \{1, \dots, d\}$	index set of features that need to be rounded
---	---

```

1 while  $\mathcal{J}^{\text{cts}} \neq \emptyset$  do
2    $\lambda^{\text{floor}(j)} \leftarrow (\lambda_1, \dots, \lfloor \lambda_j \rfloor, \dots, \lambda_d)$  for all  $j \in \mathcal{J}^{\text{cts}}$ 
3    $\lambda^{\text{ceil}(j)} \leftarrow (\lambda_1, \dots, \lceil \lambda_j \rceil, \dots, \lambda_d)$  for all  $j \in \mathcal{J}^{\text{cts}}$ 
4    $v^{\text{floor}} \leftarrow \min_{j \in \mathcal{J}} V(\lambda^{\text{floor}(j)})$ 
5    $v^{\text{ceil}} \leftarrow \min_{j \in \mathcal{J}} V(\lambda^{\text{ceil}(j)})$ 
6   if  $v^{\text{floor}} \leq v^{\text{ceil}}$  then
7      $k \leftarrow \text{argmin}_{j \in \mathcal{J}} V(\lambda^{\text{floor}(j)})$ 
8      $\lambda_k \leftarrow \lfloor \lambda_k \rfloor$ 
9   else
10     $k \leftarrow \text{argmin}_{j \in \mathcal{J}} V(\lambda^{\text{ceil}(j)})$ 
11     $\lambda_k \leftarrow \lceil \lambda_k \rceil$ 
12  end if
13   $\mathcal{J} \leftarrow \mathcal{J} \setminus \{k\}$ 
14 end while
Output:  $\lambda \in \mathcal{L}$ 

```

4.2 Narrowing the Optimality Gap

In what follows, we present two techniques that narrow the optimality gap from the lattice CP algorithm by reducing the size of the feasible region.

These techniques require *augmented* formulations of the risk score problem and its derivatives, which include new variables and constraints to bound the values of the objective function, the loss function, and ℓ_0 -norm at the optimal solution $\boldsymbol{\lambda}^*$. The augmented formulations return the same optimal solution as our earlier formulations so long as the values of V^{\min} , V^{\max} , L^{\min} , L^{\max} , R^{\min} and R^{\max} are valid.

Our goal is to solve the augmented formulations in which the values of V^{\min} , V^{\max} , L^{\min} , L^{\max} , R^{\min} and R^{\max} are as strong as possible (but still valid). By adding strong bounds, we can reduce the feasible region of these problems without discarding the optimal solution, effectively reducing the size of the search space for Algorithm 2.

AUGMENTEDRISKSCOREMINLP (\mathcal{L} , $\mathcal{H}(\theta, \boldsymbol{\lambda})$, V^{\min} , V^{\max} , L^{\min} , L^{\max} , R^{\min} , R^{\max})

$$\begin{aligned}
 & \min_{\boldsymbol{\lambda}} V \\
 \text{s.t. } & \boldsymbol{\lambda} \in \mathcal{L} \\
 & V = \theta + C_0 R \\
 & \theta = l(\boldsymbol{\lambda}) \\
 & R = \|\boldsymbol{\lambda}\|_0 \\
 & V \in [V^{\min}, V^{\max}] \\
 & \theta \in [L^{\min}, L^{\max}] \\
 & R \in [R^{\min}, R^{\max}]
 \end{aligned} \tag{6}$$

AUGMENTEDRISKSCOREMINLP (\mathcal{L} , $\mathcal{H}(\theta, \boldsymbol{\lambda})$, V^{\min} , V^{\max} , L^{\min} , L^{\max} , R^{\min} , R^{\max})

$$\begin{aligned}
 & \min_{\boldsymbol{\lambda}} V \\
 \text{s.t. } & \boldsymbol{\lambda} \in \mathcal{L} \\
 & V = \theta + C_0 R \\
 & \theta \in \mathcal{H}(\theta, \boldsymbol{\lambda}) \\
 & R = \|\boldsymbol{\lambda}\|_0 \\
 & V \in [V^{\min}, V^{\max}] \\
 & \theta \in [L^{\min}, L^{\max}] \\
 & R \in [R^{\min}, R^{\max}]
 \end{aligned} \tag{7}$$

AUGMENTEDRISKSCORELP $(\mathcal{L}, \mathcal{H}(\theta, \boldsymbol{\lambda}), V^{\min}, V^{\max}, L^{\min}, L^{\max}, R^{\min}, R^{\max})$

$$\begin{aligned}
 & \min_{\boldsymbol{\lambda}} V \\
 \text{s.t. } & \boldsymbol{\lambda} \in \mathcal{R} \\
 & V = \theta + C_0 R \\
 & \theta \in \mathcal{H}(\theta, \boldsymbol{\lambda}) \\
 & R = \sum_{j=1}^d \alpha_j \\
 & \alpha_j = \frac{\max(\lambda_j, 0)}{\Lambda_j^{\max}} + \frac{\min(\lambda_j, 0)}{\Lambda_j^{\min}} \text{ for } j = 1, \dots, d \\
 & V \in [V^{\min}, V^{\max}] \\
 & \theta \in [L^{\min}, L^{\max}] \\
 & R \in [R^{\min}, R^{\max}]
 \end{aligned} \tag{8}$$

4.2.1 CHAINED UPDATES

We will describe a simple procedure to dynamically update the values of V^{\min} , V^{\max} , L^{\min} , L^{\max} , R^{\min} and R^{\max} as the lattice CP algorithm progresses. The procedure requires no assumptions, is easy to implement, and involves minimal computation.

UNIVERSAL BOUNDS

To initialize the procedure, we use universal bounds that can be computed using the training data $(\mathbf{x}_i, y_i)_{i=1}^N$ and the coefficient set \mathcal{L} . We start with Proposition 1, which yields upper and lower bounds on the logistic loss using only the fact that the coefficient set \mathcal{L} is bounded.

Proposition 1 (Bounds on Logistic Loss over a Bounded Coefficient Set)

Let $(\mathbf{x}_i, y_i)_{i=1}^N$ denote a training dataset where $\mathbf{x}_i \in \mathcal{X} \subset \mathbb{R}^d$ and $y_i \in \mathcal{Y} = \{-1, +1\}$ for $i = 1, \dots, N$. Consider the value of the normalized logistic loss function for a linear classifier with coefficients $\boldsymbol{\lambda} \in \mathcal{L} \subset \mathbb{R}^d$

$$l(\boldsymbol{\lambda}) = \frac{1}{N} \sum_{i=1}^N \log(1 + \exp(-\langle \boldsymbol{\lambda}, y_i \mathbf{x}_i \rangle)).$$

If the coefficient set \mathcal{L} is bounded, then $l(\boldsymbol{\lambda}) \in [L^{\min}, L^{\max}]$ for all $\boldsymbol{\lambda} \in \mathcal{L}$ where

$$\begin{aligned}
 L^{\min} &= \frac{1}{N} \sum_{i:y_i=+1} \log(1 + \exp(-s_i^{\max})) + \frac{1}{N} \sum_{i:y_i=-1} \log(1 + \exp(-s_i^{\min})), \\
 L^{\max} &= \frac{1}{N} \sum_{i:y_i=+1} \log(1 + \exp(-s_i^{\min})) + \frac{1}{N} \sum_{i:y_i=-1} \log(1 + \exp(-s_i^{\max})),
 \end{aligned}$$

where $s_i^{\min} = \min_{\boldsymbol{\lambda} \in \mathcal{L}} \langle \boldsymbol{\lambda}, \mathbf{x}_i \rangle$ and $s_i^{\max} = \max_{\boldsymbol{\lambda} \in \mathcal{L}} \langle \boldsymbol{\lambda}, \mathbf{x}_i \rangle$ for $i = 1, \dots, N$.

The value of L^{\min} in Proposition 1 represents the best case loss in a perfectly separable setting when we assign each positive example the largest possible score s_i^{\max} , and each negative example i the smallest possible score s_i^{\min} . Conversely, the value of L^{\max} represents the worst case loss when we assign each positive example i with its smallest score s_i^{\min} , and each negative example i with its largest score s_i^{\max} . In practice, L^{\min} and L^{\max} can be computed in $O(N)$ flops using only the training data and the coefficient set by evaluating s_i^{\min} and s_i^{\max} for $i = 1, \dots, N$ as follows.

$$s_i^{\min} = \min_{\lambda} \sum_{j=0}^d x_{ij} \lambda_j = \sum_{j=0}^d \min_{\lambda_j} x_{ij} \lambda_j = \sum_{j=0}^d \mathbb{1}[x_{ij} > 0] x_{ij} \Lambda_j^{\min} + \mathbb{1}[x_{ij} < 0] x_{ij} \Lambda_j^{\max}, \quad (9)$$

$$s_i^{\max} = \max_{\lambda} \sum_{j=0}^d x_{ij} \lambda_j = \sum_{j=0}^d \max_{\lambda_j} x_{ij} \lambda_j = \sum_{j=0}^d \mathbb{1}[x_{ij} > 0] x_{ij} \Lambda_j^{\max} + \mathbb{1}[x_{ij} < 0] x_{ij} \Lambda_j^{\min}. \quad (10)$$

In practice, the L^{\min} bound can be useful, whereas the L^{\max} bound is too loose and likely to be discarded. For instance, if we have $\mathbf{0} \in \mathcal{L}$, then $l(\mathbf{0})$ yields a much tighter upper bound than L^{\max} . Note that L^{\min} and L^{\max} can also be strengthened in the following cases:

- If we have a non-trivial limit on the number of features (i.e., $R^{\max} < d$). In this case, the values of L^{\min} and L^{\max} are limited as s_i^{\min} and s_i^{\max} are further bounded by the limit on the number of non-zero coefficients. Here, the computation of s_i^{\min} (or s_i^{\max}) can still be carried out in $O(N)$ flops by choosing the R^{\max} smallest (or largest) terms in the left hand side of equation (9) (or (10)).
- If the training data contains multiple examples with the same features and conflicting labels. In this case, we can reduce the values of L^{\min} and L^{\max} by exploiting the fact that these examples are not separable as follows. We let $s = \sum_{i: y_i = +1, \mathbf{x}_i = \mathbf{x}^0} s_i^{\max}$ and $s = \sum_{i: y_i = -1, \mathbf{x}_i = \mathbf{x}^0} s_i^{\min}$ denote the total scores of training examples such that $\mathbf{x}_i = \mathbf{x}^0$ and $y_i = +1$ or $y_i = -1$, respectively. If $\log(1 + \exp(-s^+)) > \log(1 + \exp(-s^-))$, then we construct L^{\max} by assigning the largest score s_i^{\max} to all points i with $\mathbf{x}_i = \mathbf{x}^0$, and construct L^{\min} by assigning the smallest score s_i^{\min} to all points i with $\mathbf{x}_i = \mathbf{x}^0$ (and vice-versa if $\log(1 + \exp(-s^+)) < \log(1 + \exp(-s^-))$).

We can bound the number of non-zero coefficients R to $[0, d]$, trivially. In some problems, however, these trivial bounds are stronger due to operational constraints (e.g., if we need to fit risk scores with at most 5 features, then we $R \in [0, 5]$). Having initialized L^{\min} , L^{\max} , R^{\min} and R^{\max} , we can set the bounds on the objective values as:

$$V^{\min} = L^{\min} + C_0 R^{\min}, \quad (11)$$

$$V^{\max} = L^{\max} + C_0 R^{\max}. \quad (12)$$

PROBLEM-SPECIFIC BOUNDS FOR CHAINED UPDATES

The following propositions help us recover stronger bounds using the values of the upper bound V^{\max} and lower bound V^{\min} generated over the course of the lattice CP algorithm.

Proposition 2 (Upper Bound on Optimal Number of Non-Zero Coefficients)

Given an upper bound on the objective value $V^{\max} \geq V(\boldsymbol{\lambda}^*)$, and a lower bound on the loss function $L^{\min} \leq l(\boldsymbol{\lambda}^*)$, we can derive an upper bound on the value of the number of optimal non-zero coefficients $R^{\max} \geq \|\boldsymbol{\lambda}^*\|_0$ as

$$R^{\max} = \left\lfloor \frac{V^{\max} - L^{\min}}{C_0} \right\rfloor$$

Proposition 3 (Upper Bound on Optimal Loss)

Given an upper bound on the objective value $V^{\max} \geq V(\boldsymbol{\lambda}^*)$, and a lower bound on the number of non-zero coefficients $R^{\min} \leq \|\boldsymbol{\lambda}^*\|_0$, we can derive an upper bound on value of the loss function $L^{\max} \geq l(\boldsymbol{\lambda}^*)$ where

$$L^{\max} = V^{\max} - C_0 R^{\min}.$$

Proposition 4 (Lower Bound on Optimal Loss)

Given a lower bound on the objective value $V^{\min} \leq V(\boldsymbol{\lambda}^*)$, and an upper bound on the number of non-zero coefficients $R^{\max} \geq \|\boldsymbol{\lambda}^*\|_0$, we can derive a lower bound on value of the loss function $L^{\min} \leq l(\boldsymbol{\lambda}^*)$ where

$$L^{\min} = V^{\min} - C_0 R^{\max}.$$

CHAINED UPDATES PROCEDURE

We use Propositions 2 – 4 in a simple procedure to update the bounds used in the augmented formulations of RISKSLIMMINLP, RISKSLIMMIP and RISKSLIMLP (Algorithm 5).

Algorithm 5 Chained Update Procedure for Lattice CP Algorithm

Input

C_0	RISKSLIMMINLP ℓ_0 penalty parameter
$V^{\min}, V^{\max}, L^{\min}, L^{\max}, R^{\min}, R^{\max}$	initial bounds on $V(\boldsymbol{\lambda}^*)$, $l(\boldsymbol{\lambda}^*)$ and $\ \boldsymbol{\lambda}^*\ _0$

- 1 **repeat**
- 2 $V^{\min} \leftarrow \max(V^{\min}, L^{\min} + C_0 R^{\min})$ ▷ update lower bound on $V(\boldsymbol{\lambda}^*)$
- 3 $V^{\max} \leftarrow \min(V^{\max}, L^{\max} + C_0 R^{\max})$ ▷ update upper bound on $V(\boldsymbol{\lambda}^*)$
- 4 $L^{\min} \leftarrow \max(L^{\min}, V^{\min} - C_0 R^{\max})$ ▷ update lower bound on $l(\boldsymbol{\lambda}^*)$
- 5 $L^{\max} \leftarrow \min(L^{\max}, V^{\max} - C_0 R^{\min})$ ▷ update upper bound on $l(\boldsymbol{\lambda}^*)$
- 6 $R^{\max} \leftarrow \min\left(R^{\max}, \left\lfloor \frac{V^{\max} - L^{\min}}{C_0} \right\rfloor\right)$ ▷ update upper bound on $\|\boldsymbol{\lambda}^*\|_0$
- 7 **until** Steps 2 to 6 produce no updates

Output: $V^{\min}, V^{\max}, L^{\min}, L^{\max}, R^{\min}, R^{\max}$

Propositions 2 – 4 impose dependencies between the values of V^{\min} , V^{\max} , L^{\min} , L^{\max} , R^{\min} and R^{\max} that may lead to a complex “chain” of updates. As shown in Figure 4.2.1, it may be possible to update more than one of these values, and update some values more than once. Consider a case where we run Algorithm 5 when our MIP solver improves the

lower bound on the objective value V^{\min} . If we update the lower bound on the loss L^{\min} at Step 4, but do not update the upper bound on the ℓ_0 -norm R^{\max} at Step 6, then it will not update V^{\max} , L^{\min} , L^{\max} , V^{\min} at the next iteration. However, if R^{\max} is updated after rounding, then V^{\max} , L^{\min} , L^{\max} , V^{\min} will be updated.

In light of these dependencies, Algorithm 5 cycles through Propositions 2 – 4 until it cannot update any of the values of V^{\min} , V^{\max} , L^{\min} , L^{\max} , R^{\min} and R^{\max} . This ensures that Algorithm 5 returns the strongest possible bounds, regardless of the value that updated in the first place. In practice, this also means that we can make use of 5 in a variety of situations, such as the initialization procedure from Section 4.2.2.

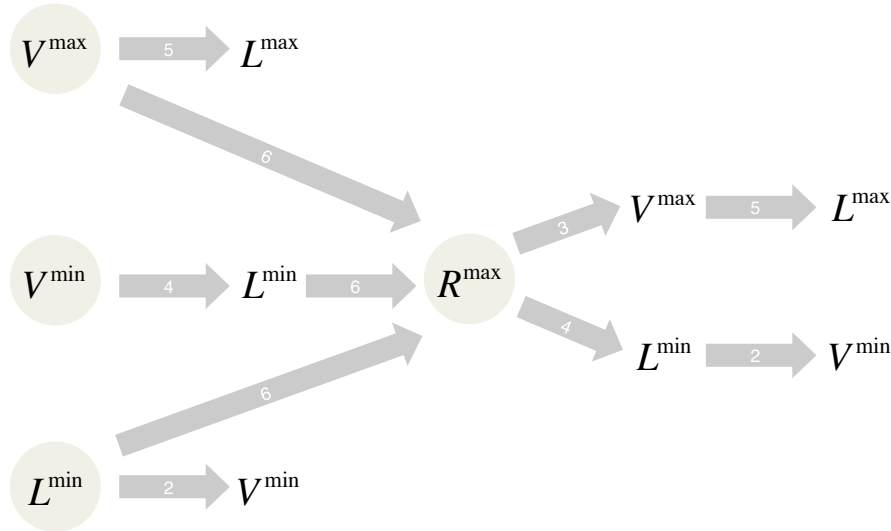


Figure 6: All possible update “chains” in Algorithm 5. We circle terms that may be updated externally by the MIP solver used in the lattice CP algorithm. If any of the circled terms are updated, we run the procedure in Algorithm 5, and potentially update all terms within the path marked by the arrows. Here, the numbers inside each arrows refer to the relevant update step in Algorithm 5.

In Figure 4.2.1, we show how the chained update procedure in Algorithm 5 can improve the lower bound and optimality gap when used in the lattice CP algorithm. Here, we run Algorithm 5 when we update the global upper bound V^{\max} in Step 9, or the global lower bound V^{\min} in Step 16. If the procedure improves one of the bounds, we pass these along to the MIP solver by updating the bounds in our formulation (see Appendix ?? for implementation details).

4.2.2 INITIALIZATION

In Algorithm 6, we present an initialization procedure to kick-start lattice CP algorithm with a high quality feasible solution, a set of initial cutting planes, and strong bounds on the optimal values of the objective function, loss function, and number of non-zero coefficients. The procedure makes use of all techniques presented so far, as follows:

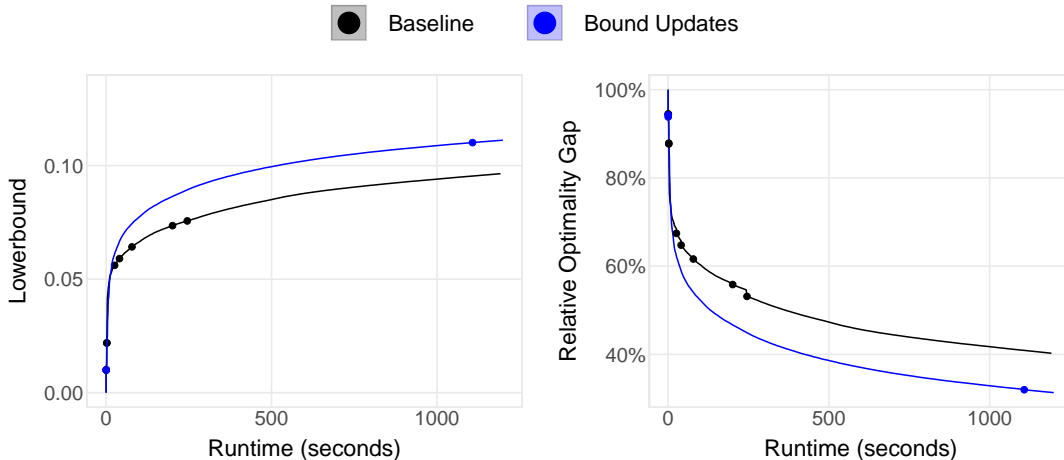


Figure 7: Performance profile of lattice CP with and without chained updates. We show the lower bound V^{\min} and the relative optimality gap $(V^{\max} - V^{\min})/V^{\max}$, and add points to mark points at which lattice CP updates the incumbent solution. Results reflect performance on a simulated dataset with $d = 30$ and $N = 50\,000$ (see Appendix B for details).

1. **Conventional CP on Convex Relaxation of RiskSlimMINLP:** We use the conventional CP algorithm to solve $\text{RISKSLIMLP}(\text{conv}(\mathcal{L}), \mathcal{H}^0(\theta, \lambda))$ (i.e the convex relaxation of RISKSLIMMINLP that uses a cutting plane approximation). We use the lower bound on the objective value of RISKSLIMLP to obtain a lower bound on the optimal objective value V^{\min} . In addition, we store the cutting planes from RISKSLIMLP to use when starting the lattice CP algorithm.
2. **Sequential Rounding and Polishing:** For each solution produced by the conventional CP algorithm, we run sequential rounding (Algorithm 4) to obtain an integer feasible solution for RISKSLIMMINLP . We then polish this solution using DCD (Algorithm 3). We use the best solution to update the upper bound on the optimal objective value V^{\max} .
3. **Chained Updates:** Having obtained strong bounds on V^{\min} and V^{\max} , we update the bounds $V^{\min}, V^{\max}, L^{\min}, L^{\max}, R^{\min}, R^{\max}$ using the chained updates procedure in Algorithm 5.

Algorithm 6 Initialization Procedure for Lattice CP

Input

$(\mathbf{x}_i, y_i)_{i=1}^N$	training data
C_0	RISKSLIMMINLP ℓ_0 penalty parameter
\mathcal{L}	RISKSLIMMINLP coefficient set
$V^{\min}, V^{\max}, L^{\min}, L^{\max}, R^{\min}, R^{\max}$	initial bounds on $V(\boldsymbol{\lambda}^*)$, $l(\boldsymbol{\lambda}^*)$ and $\ \boldsymbol{\lambda}^*\ _0$
T	time limit for conventional CP on RISKSLIMLP

Initialize

$\mathcal{H}^0(\theta, \boldsymbol{\lambda}) \leftarrow \{\theta \geq 0\}$	collection of cutting planes to the loss function
$K \leftarrow 0$	# of iterations for conventional CP on RISKSLIMLP
$\mathcal{Q} \leftarrow \emptyset$	set of feasible solutions to RISKSLIMLP (continuous)
$\mathcal{P} \leftarrow \emptyset$	set of feasible solutions to RISKSLIMMINLP (discrete)

Step I: Solve RISKSLIMLP using Conventional CP

- 1 Solve RISKSLIMLP ($\text{conv}(\mathcal{L}), \mathcal{H}^0(\theta, \boldsymbol{\lambda})$) using conventional CP ▷ Algorithm 1
- $K \leftarrow$ # of iterations completed in T seconds.
- $\mathcal{H}(\theta, \boldsymbol{\lambda}) \leftarrow \mathcal{H}^K(\theta, \boldsymbol{\lambda})$ ▷ store cutting plane from each iteration
- $\mathcal{Q} \leftarrow \{\boldsymbol{\lambda}^k\}_{k=1}^K$ ▷ store solution from each iteration

Step II: Round and Polish Continuous Solutions from Conventional CP

- 2 **for each** $\boldsymbol{\lambda}^{\text{CTS}} \in \mathcal{Q}$ **do**
- 3 $\boldsymbol{\lambda}^{\text{SR}} \leftarrow \text{SEQUENTIALROUNDING}(\boldsymbol{\lambda}^{\text{CTS}}, \mathcal{L}, C_0)$ ▷ Algorithm 4
- 4 $\boldsymbol{\lambda}^{\text{DCD}} \leftarrow \text{DISCRETECOORDINATEDDESCENT}(\boldsymbol{\lambda}^{\text{SR}}, \mathcal{L}, C_0)$ ▷ Algorithm 3
- 5 $\mathcal{P} \leftarrow \mathcal{P} \cup \boldsymbol{\lambda}^{\text{DCD}}$
- 6 **end for**
- 7 $\boldsymbol{\lambda}^{\text{best}} \leftarrow \text{argmin}_{\boldsymbol{\lambda} \in \mathcal{P}} V(\boldsymbol{\lambda})$

Step III: Update Bounds on $V(\boldsymbol{\lambda}^*)$, $l(\boldsymbol{\lambda}^*)$ and $\|\boldsymbol{\lambda}^*\|_0$

- 8 $V^{\min} \leftarrow \max(V^{\min}, \hat{V}^K(\boldsymbol{\lambda}^K))$ ▷ lower bound on RISKSLIMLP is a lower bound on $V(\boldsymbol{\lambda}^*)$
- 9 $V^{\max} \leftarrow \min(V^{\max}, V(\boldsymbol{\lambda}^{\text{best}}))$ ▷ best feasible solution is an upper bound on $V(\boldsymbol{\lambda}^*)$
- 10 $(V^{\min}, V^{\max}, L^{\min}, L^{\max}, R^{\min}, R^{\max}) \leftarrow \text{CHAINEDUPDATES}(V^{\min}, \dots, R^{\max}, C_0)$ ▷ Algorithm 5

Output: $\boldsymbol{\lambda}^{\text{best}}, \mathcal{H}(\theta, \boldsymbol{\lambda}), V^{\min}, V^{\max}, L^{\min}, L^{\max}, R^{\min}, R^{\max}$

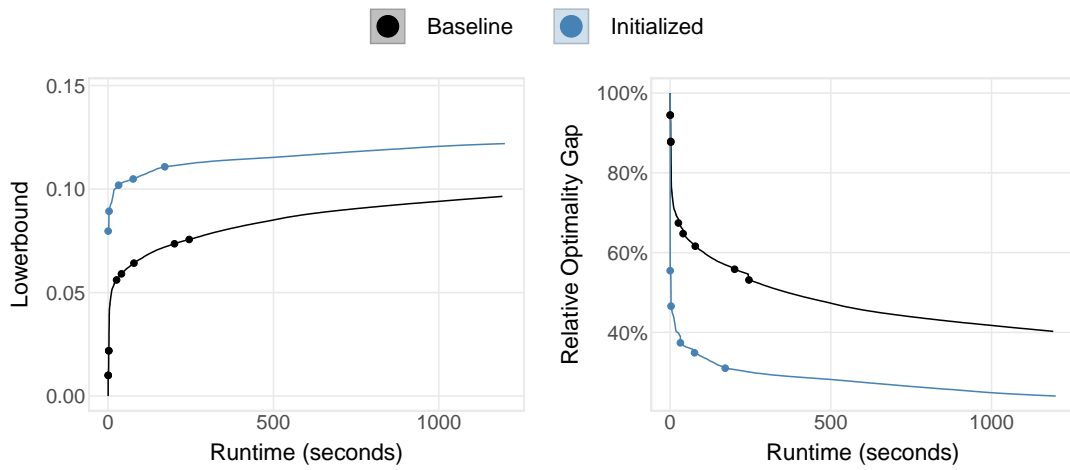


Figure 8: Performance profile of lattice CP with and without initialization. We show the lower bound V^{\min} and the relative optimality gap $(V^{\max} - V^{\min})/V^{\max}$, and add points to mark points at which lattice CP updates the incumbent solution. Results reflect performance on a simulated dataset with $d = 30$ and $N = 50\,000$ (see Appendix B for details).

5. Reducing Data-Related Computation

In this section, we present two specialized techniques to reduce data-related computation for the risk score problem by exploiting the fact that the coefficients belong to a bounded discrete set \mathcal{L} . By reducing the time spent on data-related computation, these techniques let us fit high quality models in less time, and for a larger range of datasets.

5.1 Fast Loss Evaluation via Lookup Tables

The first technique is designed to reduce the time needed to evaluate the loss function and its gradient, which are functions that are called when computing the cutting plane parameters (3), and running the heuristic procedures from Section 4.1.

This technique requires that the features $\mathbf{x}_i \in \mathcal{X}$ and coefficients $\boldsymbol{\lambda} \in \mathcal{L}$ belong to sets that are bounded, discrete, and regularly spaced, such as $\mathcal{X} \subseteq \{0, 1\}^d$ (binary features) and $\mathcal{L} \in \{-10, \dots, 10\}^{d+1}$ (bounded integer coefficients).

Evaluating the logistic loss function $\log(1 + \exp(-\langle \boldsymbol{\lambda}, y_i \mathbf{x}_i \rangle))$ for a given value of $\boldsymbol{\lambda}$ is relatively expensive in terms of computation because it involves exponentiation, and because it needs to be implemented in multiple steps in order to avoid numerical overflow/underflow when the score $s_i := \langle \boldsymbol{\lambda}, \mathbf{x}_i y_i \rangle$ is too small or large³.

Since the points in the training data $(\mathbf{x}_i, y_i)_{i=1}^N$ belong to a bounded and discrete set $\mathcal{D} \subseteq (\mathcal{X} \times \mathcal{Y})^N$, and the coefficients $\boldsymbol{\lambda}$ belong to a discrete and bounded set \mathcal{L} , then the scores $s_i = \langle \boldsymbol{\lambda}, \mathbf{x}_i y_i \rangle$ also belong to a discrete and bounded set

$$\mathcal{S} = \{ \langle \boldsymbol{\lambda}, \mathbf{x}_i y_i \rangle \mid i = 1, \dots, N \text{ and } \boldsymbol{\lambda} \in \mathcal{L} \}.$$

If the elements of the feature set \mathcal{X} and the coefficients set \mathcal{L} are regularly spaced (say with spacing 1), then the scores will belong to the set of integers $\mathcal{S} \subseteq \mathbb{Z} \cap [s^{\min}, s^{\max}]$ where:

$$s^{\min} = \min_{i, \boldsymbol{\lambda}} \{ \langle \boldsymbol{\lambda}, \mathbf{x}_i y_i \rangle \text{ for all } (\mathbf{x}_i, y_i) \in \mathcal{D} \text{ and } \boldsymbol{\lambda} \in \mathcal{L} \}$$

$$s^{\max} = \max_{i, \boldsymbol{\lambda}} \{ \langle \boldsymbol{\lambda}, \mathbf{x}_i y_i \rangle \text{ for all } (\mathbf{x}_i, y_i) \in \mathcal{D} \text{ and } \boldsymbol{\lambda} \in \mathcal{L} \}$$

Thus, we can precompute and store all possible values of the loss function in a lookup table with $s^{\max} - s^{\min} + 1$ rows, where row m contains the value of $\lceil \log(1 + \exp(-(m + s^{\min} - 1))) \rceil$.

This strategy can reduce the time needed to evaluate the loss function as we replace a computationally expensive operation with a simple lookup operation. In practice, the lookup table is usually small enough to be cached in memory, which yields a substantial runtime speedup. Further, since the values of s^{\min} and s^{\max} can be computed exactly in $O(N)$ time, the lookup table can be narrowed down as R^{\max} is updated over the course of the lattice CP algorithm.

As shown in Figure ??, the lookup table reduces the total amount of data-related computation compared to a standard high performance numerical computation library. The reduction in data-related computation may translate into a significant difference in the ability of the algorithm to return a high quality risk score, with a stronger proof of optimality under a time constraint.

3. The value of $\exp(-s_i) = \exp(-\langle y_i \mathbf{x}_i, \boldsymbol{\lambda} \rangle)$ can be computed reliably using IEEE 754 double precision floating point numbers when s_i is roughly between -700 and 700. The term will overflow to ∞ when $s_i < -700$, and underflow to 0 when $s_i > 700$.

5.2 Cheaper Heuristics via Subsampling

The next technique is aims to reduce data-related computation for heuristic procedures such as sequential rounding by using a subsample of the full training dataset.

In theory, we wish to run heuristic procedures frequently as they can yield feasible solutions to RISKSLIMMINLP. In practice, however, we limit the number of times we run these procedures because each run requires multiple evaluations of the loss function, and runs that fail to update the incumbent solution effectively slow down the progress of the lattice CP algorithm. If, for example, we ran sequential rounding each time we found a new set of continuous coefficients in the lattice CP algorithm, then we would spend too much time rounding, without necessarily finding a better solution.

The technique works as follows. Before running the lattice CP algorithm, we set aside a “heuristics” dataset \mathcal{D}_M by sampling M points without replacement from the full training dataset \mathcal{D}_N . Once we run the lattice CP algorithm, we then reduce data-related computation by running all heuristics using \mathcal{D}_M . To distinguish between situations where the loss and objective are computed with \mathcal{D}_M or \mathcal{D}_N , let $l_i(\boldsymbol{\lambda}) = \log(1 + \exp(\langle \boldsymbol{\lambda}, y_i \mathbf{x}_i \rangle))$ and define:

$$\begin{aligned} l_M(\boldsymbol{\lambda}) &= \frac{1}{M} \sum_{i=1}^M l_i(\boldsymbol{\lambda}), & V_M(\boldsymbol{\lambda}) &= l_M(\boldsymbol{\lambda}) + C_0 \|\boldsymbol{\lambda}\|_0 \\ l_N(\boldsymbol{\lambda}) &= \frac{1}{N} \sum_{i=1}^N l_i(\boldsymbol{\lambda}), & V_N(\boldsymbol{\lambda}) &= l_N(\boldsymbol{\lambda}) + C_0 \|\boldsymbol{\lambda}\|_0. \end{aligned}$$

Consider a case where a heuristic procedure returns a “promising” solution $\boldsymbol{\lambda}^H$ such that:

$$V_M(\boldsymbol{\lambda}^H) < V^{\max}. \quad (13)$$

In this case, we compute the objective value on the full training dataset \mathcal{D}_N by evaluating the loss at each of the $N - M$ points that were not included in \mathcal{D}_M . As usual, we then update the incumbent solution if $\boldsymbol{\lambda}^H$ attains an objective value that is less than the current upper bound on RISKSLIMMINLP:

$$V_N(\boldsymbol{\lambda}^H) < V^{\max} \quad (14)$$

Note that although we always evaluate the loss for the full training dataset \mathcal{D}_N to confirm an incumbent update, this technique still reduces data-related computation as heuristic procedures typically require us to evaluate the loss multiple times (e.g., sequential rounding requires $\frac{1}{3}d(d^2 - 1)$ evaluations of the loss). In the interest of reducing computation, this technique also ignores “false negative” solutions $\boldsymbol{\lambda}^H$ that do poorly on the heuristics dataset $V_M(\boldsymbol{\lambda}^H) \geq V^{\max}$ but would update the incumbent on the true dataset $V_N(\boldsymbol{\lambda}^H) < V^{\max}$.

The main draw of using the subsampling technique is the following generalization bound that guarantees that any solution that updates the incumbent when the objective is evaluated with \mathcal{D}_M will also update incumbent when the objective is evaluated with \mathcal{D}_N (i.e., that any solution that satisfies (13) will also satisfy (14)).

Theorem 1 (Generalization of Sampled Loss on Finite Coefficient Set)

Let $\mathcal{D}_N = (\mathbf{x}_i, y_i)_{i=1}^N$ denote a training dataset with $N > 1$ points, and let $\mathcal{D}_M = (\mathbf{x}_i, y_i)_{i=1}^M$ denote a sample of M points drawn without replacement from \mathcal{D}_N . Let $\boldsymbol{\lambda}$ denote the coefficients of a linear classifier from a finite set \mathcal{L} . For all $\varepsilon > 0$, it holds that

$$\Pr \left(\max_{\boldsymbol{\lambda} \in \mathcal{L}} (l_N(\boldsymbol{\lambda}) - l_M(\boldsymbol{\lambda})) \geq \varepsilon \right) \leq |\mathcal{L}| \exp \left(- \frac{2\varepsilon^2}{\left(\frac{1}{M}\right)\left(1 - \frac{M}{N}\right)\left(1 + \frac{M}{N}\right)\Delta^{\max}(\mathcal{L}, \mathcal{D}_N)^2} \right)$$

where

$$\Delta^{\max}(\mathcal{L}, \mathcal{D}_N) = \max_{\boldsymbol{\lambda} \in \mathcal{L}} \left(\max_{i=1, \dots, N} l_i(\boldsymbol{\lambda}) - \min_{i=1, \dots, N} l_i(\boldsymbol{\lambda}) \right)$$

Theorem 1 is a generalization bound that is derived from a concentration inequality for problems where we are sampling without replacement, known as the Hoeffding-Serfling inequality (see Bardenet et al., 2015). The Hoeffding-Serfling inequality can be significantly tighter than the classical Hoeffding inequality as it ensures that $\Pr (l_N(\boldsymbol{\lambda}) - l_M(\boldsymbol{\lambda}) \geq \varepsilon) \rightarrow 0$ as $M \rightarrow N$ for all $\varepsilon > 0$. Here, $\Delta^{\max}(\mathcal{L}, \mathcal{D}_N)$ is a normalization term that represents the maximum range of loss values on the full training dataset \mathcal{D}_N for the coefficient set \mathcal{L} . This term can be computed cheaply using the smallest and largest values of the coefficients and features as shown in Proposition 1 (Section 4.2.1).

In general, the $|\mathcal{L}|$ term in Theorem 1 produces a bound that is too loose to be useful. In the case of rounding heuristics, however, it effectively limits the difference between $l_N(\boldsymbol{\lambda})$ and $l_M(\boldsymbol{\lambda})$ since the feasible coefficient set \mathcal{L} contains at most 2^d possible values. In this setting, Theorem 1 can be used to assess the probability that a proposed incumbent update will lead to an actual incumbent update, as shown in Corollary 1. Alternatively, it can be used to choose the size of the subsampled dataset M so as to guarantee that an incumbent update on \mathcal{D}_M will yield an incumbent update on \mathcal{D}_N . In either case, the bound can be strengthened by recomputing the normalization term $\Delta^{\max}(\mathcal{L}(\boldsymbol{\rho}), \mathcal{D}_N)$ separately for each continuous solution $\boldsymbol{\rho}$, or periodically over the course of the lattice CP algorithm (as the MIP solver reduces the set of feasible coefficients via branch-and-bound).

Corollary 1 (Update Probabilities of Rounding Heuristics on Sampled Data)

Consider a rounding heuristic that takes as input a vector of continuous coefficients $\boldsymbol{\rho} = (\rho_1, \dots, \rho_d) \in \text{conv}(\mathcal{L})$ and produces as output a vector of integer coefficients $\boldsymbol{\lambda} \in \mathcal{L}(\boldsymbol{\rho})$ where

$$\mathcal{L}(\boldsymbol{\rho}) = \left\{ \boldsymbol{\lambda} \in \mathcal{L} \mid \lambda_j \in \{ \lceil \rho_j \rceil, \lfloor \rho_j \rfloor \} \text{ for } j = 1, \dots, d \right\}$$

Consider evaluating the rounding heuristic using a sample of M points $\mathcal{D}_M = (\mathbf{x}_i, y_i)_{i=1}^M$ drawn without replacement from the full training dataset $\mathcal{D}_N = (\mathbf{x}_i, y_i)_{i=1}^N$. Pick a tolerance $\delta > 0$. Given rounded coefficients $\boldsymbol{\lambda} \in \mathcal{L}(\boldsymbol{\rho})$, compute $V_M(\boldsymbol{\lambda})$. If

$$V_M(\boldsymbol{\lambda}) < V^{\max} - \varepsilon_\delta,$$

then w.p. at least $1 - \delta$, we have

$$V_N(\boldsymbol{\lambda}) \leq V^{\max}$$

where

$$\varepsilon_\delta = \Delta^{\max}(\mathcal{L}(\boldsymbol{\rho}), \mathcal{D}_N) \sqrt{\frac{\log(1/\delta) + d \log(2)}{2} \left(1 - \frac{M}{N}\right) \left(1 + \frac{M}{N}\right)}.$$

6. Benchmarking Experiments

In this section, we benchmark methods in terms of their ability to create sparse risk scores with small integer coefficients. In addition to our proposed approach to creating optimized risk scores by solving RISKSLIMMINLP, we consider a principled heuristic approach that rounds the coefficients from sparse logistic regression, as well as improved versions of this approach that make use of the rounding and polishing techniques we present in Section 4.

6.1 Experimental Setup

6.1.1 DATASETS

We ran experiments on 6 publicly available datasets listed in Table 2. Other than the `arrest` dataset, all datasets can be downloaded from the UCI Machine Learning repository (Lichman, 2013). The `arrest` dataset is also publicly available but must be formally requested from the U.S. Department of Justice, Bureau of Justice Statistics (2014). We chose these datasets to explore the performance of each method as we varied the size and nature of the training data. We processed each dataset by binarizing all categorical features and some real-valued features. For the purposes of reproducibility, we include all processed datasets other than `arrest` along with our final submission.

Dataset	Source	Classification Task
<code>adult</code>	Kohavi (1996)	predict if a U.S. resident earns more than \$50 000
<code>arrest</code>	Zeng et al. (2015)	predict if a prisoner will be arrested within 3 years of release
<code>bank</code>	Moro et al. (2014)	predict if person signs up for bank account after marketing call
<code>cancer</code>	Mangasarian et al. (1995)	detect breast cancer from a biopsy
<code>mushroom</code>	Schlimmer (1987)	predict if a mushroom is poisonous
<code>spambase</code>	Cranor and LaMacchia (1998)	predict if an e-mail is spam

Table 2: Datasets used in the benchmarking experiments.

6.1.2 METHODS

For each dataset, we fit a risk score model with small integer coefficients between (i.e., $\lambda_j \in [-5, 5]$) and a limited model size (i.e., $\|\boldsymbol{\lambda}\|_0 \leq 5$). Our choice was designed to produce risk scores similar to those that are used in practice (see e.g., the CHADS₂ score of Gage et al., 2001). In addition to our proposed method (which fits optimal risk scores), we also used: standard penalized logistic regression (as a baseline, as it obeys the model size constraint but not the integrality constraint); and 6 heuristic methods that round the coefficients from penalized logistic regression (using either simple techniques used in practice, and/or the techniques from Section 4). In what follows, we provide details on each method.

- **Optimized Risk Score (RISKSLIM):** We solved RISKSLIMMINLP using the lattice CP algorithm along with proposed improvements in Sections 4 and 5 (see Appendix ?? for implementation details). We solved each instance of RISKSLIMMINLP for 20 minutes using CPLEX 12.6.3 on 3.33GHz Intel Xeon CPU with 16GB of RAM.

- **Penalized Logistic Regression (PLR)**: We fit logistic regression models with a combined ℓ_1/ℓ_2 penalty using the glmnet package in R 3.2.3 (Friedman et al., 2010; R Core Team, 2014) (i.e. generalized linear model with a binomial link function and an elastic net penalty). We considered models for 1100 parameter instances (11 values of $alpha \in \{0.0, 0.1, \dots, 1.0\} \times 100$ values of $lambda$ chosen automatically by glmnet, where $alpha$ is the elastic-net mixing parameter and $lambda$ is the regularization penalty). In addition, we added upper and lower bounds to constrain coefficients between -5 and 5.
- **PLR + Naive Rounding (RD)**: We fit a pool of PLR models as described above. For each model in the pool, we round the coefficients to their nearest value in $\{-5, \dots, 5\}^d$ (i.e., $\lambda_j \leftarrow \lceil \min(\max(\lambda_j, -5), 5) \rceil$ for $j = 1, \dots, d$). The coefficient for the intercept is rounded to the nearest integer (i.e., $\lambda_0 \leftarrow \lceil \lambda_0 \rceil$).
- **PLR + Rescaled Rounding (RSRD)**: We fit a pool of PLR models as described above. For each model in the pool, we first rescale the coefficients for all variables so that the largest coefficient is 5 and then round to the nearest integer (i.e., $\lambda_j \rightarrow \lceil \gamma \lambda_j \rceil$ where $\gamma = 5 / \max_{j=1, \dots, d} (|\lambda_j|)$). Here, the rescaling is meant to prevent the method from setting coefficients to zero when they are between $[-0.5, 0.5]$. As before, the coefficient for the intercept is rounded to the nearest integer (i.e., $\lambda_0 \leftarrow \lceil \lambda_0 \rceil$).
- **PLR + Sequential Rounding (SEQRD)**: We fit a pool of PLR models as described above. For each model in the pool, we round the coefficients using sequential rounding (Algorithm 4 in Section 4.1.2).
- **Polished Versions of PLR (RD*, RSRD*, SEQRD*)**: We use one of the three rounding methods described above (RD, RSRD, or SEQRD) and then polish the coefficients using discrete coordinate descent (DCD; Algorithm 3 in Section 4.1.1). To guarantee that the number of non-zero coefficients does not increase (which would violate the model size requirement), we only run DCD on the set of non-zero coefficients (i.e. j such that $\lambda_j \neq 0$ where λ_j is the coefficient for variable j).

6.1.3 MODEL SELECTION

We used a standard nested 5-fold cross-validation (5-CV) to select a suitable final model and assess its predictive accuracy. We fit a final model using all of training data. The free parameters for this model were chosen as the instance that: (i) satisfied the model size constraint; and (ii) maximized the “outer” 5-CV mean test AUC. Since this tuning procedure involves 5-CV statistics in step (ii), the 5-CV statistics of the chosen model are optimistically biased. To avoid this bias, we constructed the 5-CV estimates we report by running the same model selection procedure within each fold using an “inner” 5-CV. Explicitly, for each of the 5 outer folds, we ran an inner 5-CV, and then picked a representative model for that fold by choosing the free parameter instance that: (i) satisfied the model size constraint; and (ii) maximized the “outer” 5-CV mean test AUC.

Note that model selection is not required for RiskSLIM since it can fit a model that obeys sparsity and integrality constraints without parameter tuning (e.g., to fit a model with a coefficients between -5 to 5 and 5 features by adding a constraint on the ℓ_0 norm to 5 and setting C_0 to a very small value).

6.1.4 PERFORMANCE METRICS

We evaluated all risk score models in terms of the following criteria:

- Rank Accuracy: We used the standard area under the receiver operator characteristic curve (AUC).
- Risk Calibration: We constructed *reliability diagrams* which plot, for each distinct score, the predicted probability on the x-axis against the true probabilities on the y-axis⁴ (see DeGroot and Fienberg, 1983). We summarize how well the predicted probabilities match the true probabilities through the *calibration error* (CAL), defined as the mean squared error between the predicted probability and the true probabilities (see e.g., Caruana and Niculescu-Mizil, 2006). When a risk score model is perfectly calibrated, the predicted probabilities should match the true probabilities (i.e, the points on the reliability diagram should fall on the 45 degree line), and CAL should equal 0.0%.
- Sparsity: We used a metric known as *model size*, which represents the number of non-zero coefficients and does not count the coefficient for the intercept.

6.2 Experimental Results

In Table 3, we show performance metrics for risk scores from all methods on all datasets. In Figure 9, we include reliability diagrams for the risk scores in Table 3. In Figures 10 and 11, we include regularization plots to show AUC and CAL to show how risk scores change according to the model size limit. In Figures 12 to 14, we show examples of risk scores for `arrest`, `adult` and `bank built` using our proposed approach. In what follows, we briefly discuss several observations regarding these results.

ON THE PERFORMANCE OF RISKSLIM MODELS

As shown in Table 3, the rank accuracy and risk calibration of models changes with the value of the loss function. RISKSLIM generally produces models with lowest value of the loss. This directly translates into good performance in terms of AUC and CAL. As shown in Figures 10 and 11, the relative performance advantage of RISKSLIM models in terms of AUC and CAL is more significant at small model sizes, which is as risk scores that are used in practice almost always have a small number of features. We attribute this to the use of the ℓ_0 penalty for feature selection compared to the joint ℓ_1/ℓ_2 penalty used in PLR. The relative performance advantage of the RISKSLIM models compared to unconstrained PLR models suggests that the regularization effects of using small bounded coefficients is negligible at small model sizes.

4. Since the true probabilities are not available to us, we estimate the true probabilities for each distinct score using the empirical probabilities $\frac{1}{|\mathcal{I}(s)|} \sum_{i \in \mathcal{I}(s)} \mathbb{1}[y_i = +1]$ where $\mathcal{I}(s) = \{i \in 1, \dots, N \mid s = s_i\}$ and s_i is the score for that model. For clarity, when a method produces a risk score model with over 100 distinct scores (which happens when the data contains real-valued features), we bin together points in their predicted probabilities using 10 equally spaced bins from 0 to 1.

ON COMPUTATION AND OPTIMALITY

Although the optimization problem we need to solve to fit RISKSLIM models is \mathcal{NP} -hard, we were able to fit high-performing RISKSLIM models and obtain a certificate of optimality for all datasets in 20 minutes by using the lattice CP algorithm and the techniques in Sections 4 and 5.

RISKSLIM is the only method to pair models with a measure of optimality. Among the 6 datasets, RISKSLIM returned a full guarantee of optimality for 2 of 6 datasets, and a optimality gap of $< 10\%$ for 5 of 6 datasets. In practice, small optimality gaps suggest that RISKSLIM has fit the best possible model in the model class. Thus, if a risk score model with a small optimality gap performs poorly, users can attribute the poor performance to the model class and improve performance by fitting from a larger class of models (i.e., with a greater limit on the number of features or a broader range of coefficients). In contrast, other methods do not provide users with an optimality gap, so that when risk score models perform poorly, users cannot tell if this is because the model class is restricted or because the method they have used does not find the best possible model.

Our experience also highlighted some practical computational benefits of RISKSLIM that are difficult to measure. In particular, RISKSLIM can fit models with arbitrary constraints without tuning free parameters. This avoids the need for nested cross-validation, which can be expensive and difficult to implement depending on the size of the free parameter grid and the outcome metric used for model selection. Here, we used the 5-CV AUC for model selection, which meant that we had to compute AUC for every instance that we trained (i.e., over 6 instances for RISKSLIM vs. 33'000 instances for the remaining methods). In practice, the resulting process could take far longer than the 20 minutes needed for RISKSLIM, especially on large datasets.

ON PERFORMANCE AND PITFALLS OF ROUNDING METHODS

Our results show that existing rounding methods can have inconsistent performance. In some cases, the models produced by simply rounding the coefficients to the nearest integer can do well (see e.g, the RD models for `bank`). In other cases, performance can falter (see e.g, the RD models for `cancer`). In general, our experience suggests the performance of rounded models depends on the dataset, the sparsity requirement, and the exact method that is used for rounding. Specifically, rounding procedures work well on datasets that contain binary variables exclusively (e.g. `adult`, `arrest`, `bank`), and could do poorly when a dataset contains real-valued features.

One common reason why rounding methods fail is that they are used on models where the coefficients for important variables range between 0 to 0.5. In such cases, simple rounding (RD) sets these variables to 0, removing them from consideration (see e.g., RD results for `cancer`). One potential solution is to rescale the coefficients before rounding (RSRD). This approach has the effect of improving AUC (as it spaces out the coefficients) but dramatically affects risk calibration as the logit function is not scale invariant (see e.g., the calibration plots for RSRD in 9).

Potential ways to mitigate this pitfall include: (i) using a smarter rounding procedure (see e.g. SEQRD); (ii) polishing the results from the rounding procedure (see e.g, RD*, RSRD*, SEQRD*); (iii) running model selection after rounding, which preserves a large

pool of models from which to choose (say we were to run any model selection procedure on the pool of PLR models, and then round the coefficients from that model, then we could dramatically alter the value of the loss, and thereby also alter the performance in terms of AUC and/or CAL).

The fact that rounding methods do not provide an optimality gap is problematic, especially as they may inconsistent performance. In particular, it may be difficult to tell model is performing poorly due to a stringent set of constraints or a poorly designed rounding procedure. This issue is aggravated by the fact that the natural baseline to use for rounded models (i.e., an unrounded PLR model) tends to overfit and may perform worse than a rounded model.

Dataset	Details	Metric	PLR	RD	RSRD	SEQRD	RD*	RSRD*	SEQRD*	RISKSLIM
adult	$N = 32561$ $d = 36$	test AUC	0.817	0.845	0.835	0.830	0.841	0.854	0.832	0.854
		test CAL	5.5%	3.0%	12.3%	4.3%	5.4%	3.1%	4.2%	2.4%
		model size	4	5	5	4	5	5	4	5
		loss value	0.451	0.392	0.525	0.417	0.434	0.383	0.417	0.385
		opt. gap	-	-	-	-	-	-	-	9.7%
arrest	$N = 22530$ $d = 48$	test AUC	0.700	0.676	0.699	0.691	0.693	0.676	0.677	0.694
		test CAL	7.5%	5.2%	20.6%	5.7%	8.2%	1.4%	3.8%	1.8%
		model size	5	4	5	5	5	4	4	5
		loss value	0.638	0.618	1.194	0.626	0.654	0.618	0.624	0.610
		opt. gap	-	-	-	-	-	-	-	4.2%
bank	$N = 41188$ $d = 57$	test AUC	0.725	0.759	0.774	0.759	0.749	0.760	0.760	0.760
		test CAL	2.2%	1.9%	9.3%	1.4%	6.6%	1.3%	1.3%	1.3%
		model size	2	4	4	5	2	4	5	5
		loss value	0.339	0.292	0.767	0.289	0.381	0.289	0.289	0.289
		opt. gap	-	-	-	-	-	-	-	3.5%
cancer	$N = 683$ $d = 9$	test AUC	0.993	0.770	0.993	0.984	0.993	0.770	0.984	0.991
		test CAL	10.6%	23.4%	4.7%	5.5%	3.4%	8.0%	4.5%	3.5%
		model size	5	1	5	2	5	1	2	5
		loss value	0.163	1.073	0.581	0.199	0.353	0.347	0.136	0.113
		opt. gap	-	-	-	-	-	-	-	0.0%
mushroom	$N = 8124$ $d = 113$	test AUC	0.976	0.984	0.977	0.973	0.978	0.986	0.978	0.989
		test CAL	20.9%	12.3%	8.5%	12.3%	3.6%	4.2%	5.0%	1.8%
		model size	5	4	3	5	3	4	5	5
		loss value	0.362	0.211	0.247	0.200	0.197	0.128	0.144	0.069
		opt. gap	-	-	-	-	-	-	-	0.0%
spambase	$N = 4601$ $d = 57$	test AUC	0.823	0.910	0.862	0.908	0.867	0.913	0.908	0.906
		test CAL	10.5%	24.7%	23.6%	15.9%	21.0%	10.3%	8.3%	8.2%
		model size	4	5	5	5	5	5	5	5
		loss value	0.553	0.624	5.670	0.472	5.035	0.381	0.402	0.366
		opt. gap	-	-	-	-	-	-	-	36.0%

Table 3: Performance of risk scores produced by different methods. Here: **test AUC** is the 5-CV mean test AUC; *test CAL* is the 5-CV mean test calibration error; *model size* is the model size of the final model; *loss value* is the value of the logistic loss function for the final model; *opt. gap* is the optimality gap of the final model. Results reflect the models from each method when free parameters are chosen to maximize the 5-CV mean test AUC.

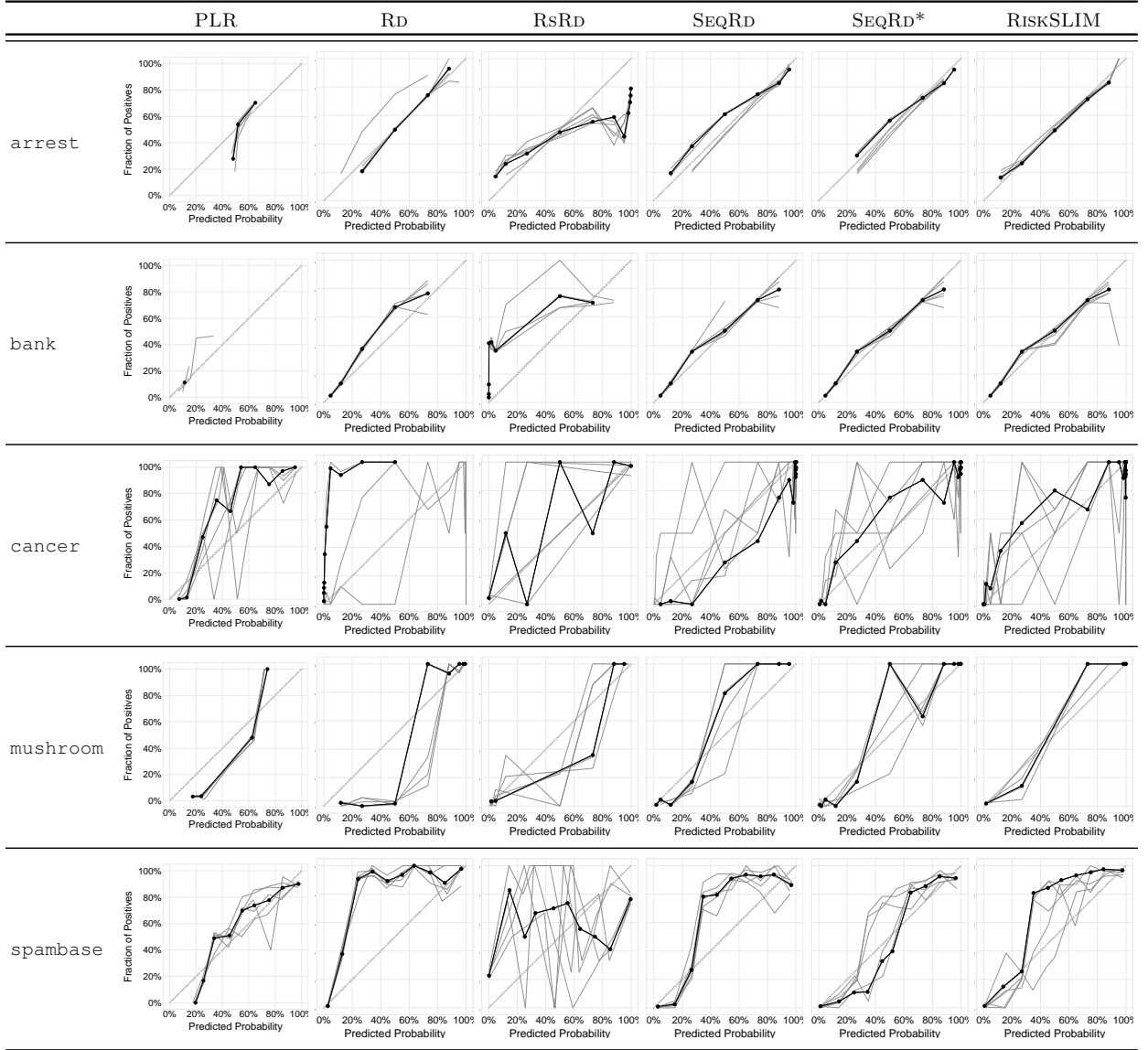


Figure 9: Reliability diagrams showing the predicted probabilities vs. observed probabilities for the best risk score with model size $\|\lambda\|_0 \leq 5$ and integer coefficients $\lambda_j \in \{-5, \dots, 5\}$ ($\lambda_j \in [-5, 5]$ for PLR). We plot results for the final model on training data in black, and results for the fold models on test data in grey.

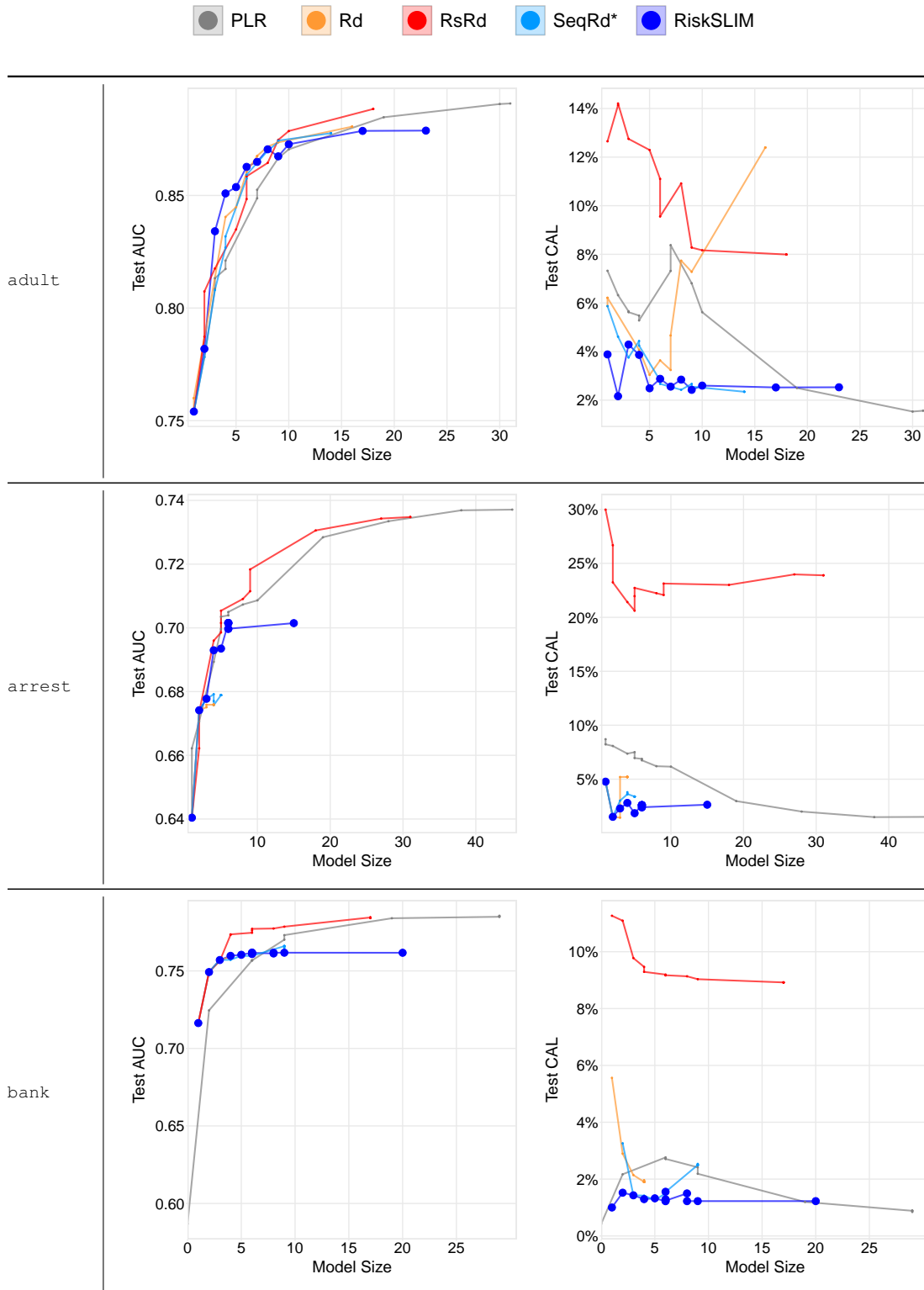


Figure 10: Test AUC (left) and test CAL (right) for risk scores with integer coefficients $\lambda_j \in \{-5, \dots, 5\}$ at model sizes between 1 to d .

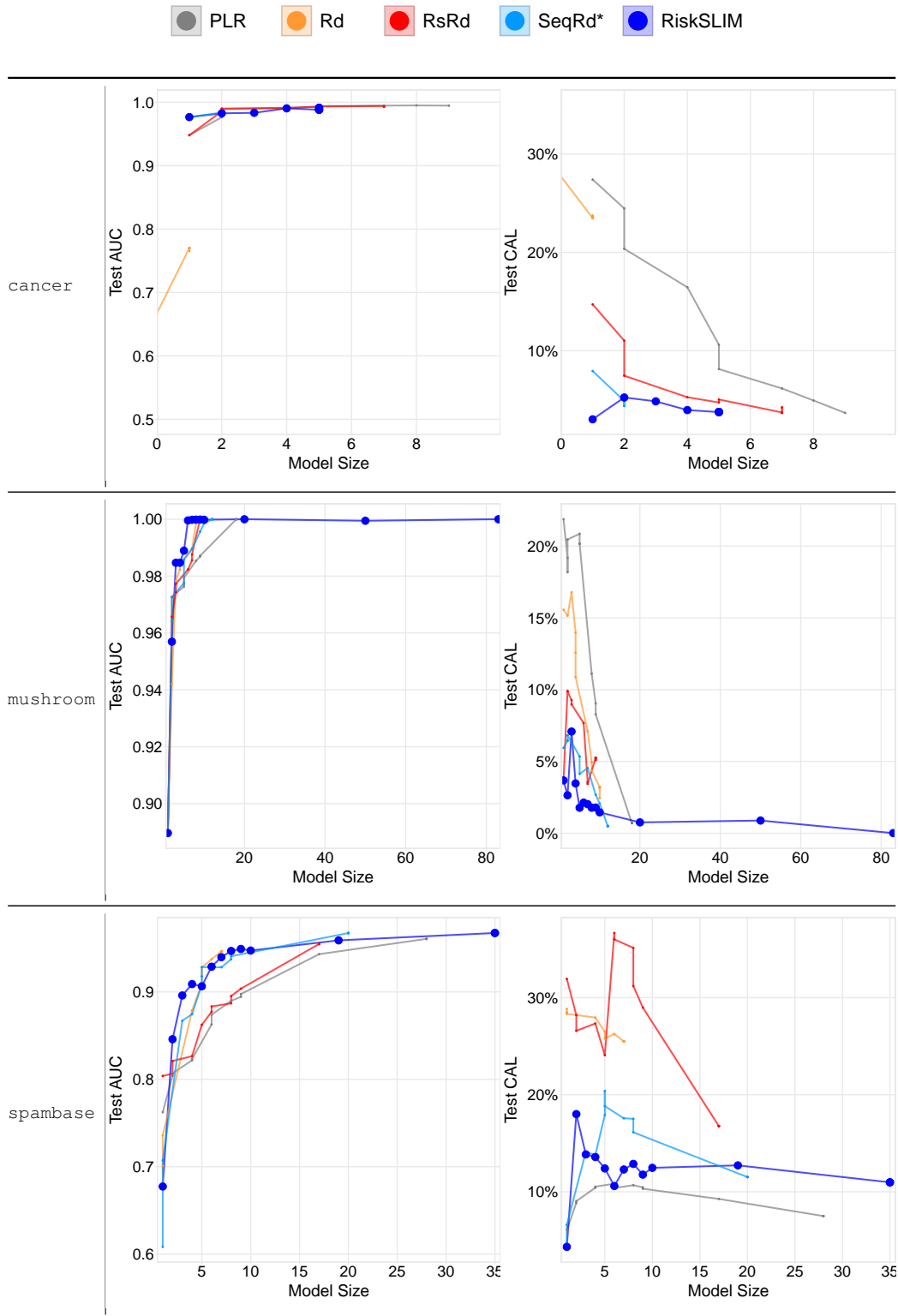


Figure 11: Test AUC (left) and test CAL (right) for risk scores with integer coefficients $\lambda_j \in \{-5, \dots, 5\}$ at model sizes between 1 to d .

1.	<i>Prior Arrests</i> ≥ 1	1 point
2.	<i>Prior Arrests</i> ≥ 5	1 point	+
3.	<i>Age at Release between 25 to 29</i>	-1 point	+
4.	<i>Age at Release between 30 to 39</i>	-1 point	+
5.	<i>Age at Release</i> ≥ 40	-2 points	+
ADD POINTS FROM ROWS 1 –5		SCORE	=

SCORE	-2	-1	0	1	2
RISK	11.9%	26.9%	50.0%	73.1%	88.1%

Figure 12: RISKSLIM model for *arrest*. RISK represents the predicted probability that a prisoner will be arrested for any offense within 3 years of release from prison. This model has a 5-CV mean test AUC/CAL of 0.694/1.8% and training AUC/CAL of 0.694/1.6%.

1.	<i>Married</i>	3 points
2.	<i>Reported Capital Gains</i>	2 points	+
3.	<i>Age between 22 to 29</i>	-1 point	+
4.	<i>Highest Level of Education is High School Diploma</i>	-2 points	+
5.	<i>No High School Diploma</i>	-3 points	+
ADD POINTS FROM ROWS 1 –5		SCORE	=

SCORE	≤ -1	0	1	2	3	4	5
RISK	5.0%	11.9	26.9%	50.0%	73.1%	88.1%	95.3

Figure 13: RISKSLIM model for *adult*. RISK represents the predicted probability that a US resident makes over \$50 000. This model has a 5-CV mean test AUC/CAL of 0.854/2.4% and training AUC/CAL of 0.860/4.1%.

1.	<i>Call between January and March</i>	1 point
2.	<i>Called Previously</i>	1 point	+
3.	<i>Previous Call was Successful</i>	1 point	+
4.	<i>Employment Indicator</i> < 5100	1 point	+
5.	<i>3 Month Euribor Rate</i> ≥ 100	-1 point	+
ADD POINTS FROM ROWS 1 –5		SCORE	=

SCORE	-1	0	1	2	3	4
RISK	4.7%	11.9	26.9%	50.0%	73.1%	88.1%

Figure 14: RISKSLIM model for *bank*. RISK represents the probability that a client will sign up for a new bank account after a marketing call. This model has a 5-CV mean test AUC/CAL of 0.760/1.3% and a training AUC/CAL of 0.760/1.1%.

7. Discussion

Our goal in this paper was to develop a new principled approach to train risk scores, which are models that are used extensively in high-stakes but are currently built ad hoc.

Our approach which recovers a simple risk score that is optimized for feature selection, small integer coefficients, and operational constraints. As shown through our results in 6, finding an optimal model leads to improved AUC and risk-calibration, especially when fitting from constrained model classes.

The discrete optimization approach that we use also leads to key practical benefits. Using discrete variables and constraints, users can fit models that obey complex operational constraints without parameter tuning and dramatically simplify the training process. When working with such constraints, the optimality gap produced through our approach is also crucial, as it allows users to tell if poor performance is due to the model class or the fitting process. An interesting line of research is to formulate operational constraints for transfer learning (see e.g., Pan and Yang, 2010).

A major part of our paper focuses on developing a cutting plane method that does not stall on non-convex problems, and pairing this method with techniques to generate feasible solutions, narrow the optimality gap, and reduce data-related computation. An important characteristic of our proposed improvements is that they are more powerful when used together. For instance, using sequential rounding and polishing to generate a feasible solution can lead to a tighter bound on the number of features through chained updates, which can then lead to faster computation by reducing the size of the lookup table.

The lattice CP algorithm that we used to solve the risk score problem can easily be adapted to solve optimization problems in which the loss function is convex, but the regularizer and feasible region are non-convex. For problems where the regularizer and feasible region are discrete, this allows users to train models in a way that scales linearly in N using a commercial MIP solver. Accordingly, an interesting direction for future work is to apply lattice CP to other supervised learning problems from this class, ℓ_0 -regularized linear regression, or problems that minimize the hinge loss over a small set of integers (Chevaleyre et al., 2013; Carrizosa et al., 2016).

Acknowledgments

We would like to thank Paul Rubin for many helpful discussions, and gratefully acknowledge support from Siemens and Wistron.

References

- Atkinson, David S and Pravin M Vaidya. A cutting plane algorithm for convex programming that uses analytic centers. *Mathematical Programming*, 69(1-3):1–43, 1995.
- Austin, James, Roger Ocker, and Avi Bhati. Kentucky pretrial risk assessment instrument validation. *Bureau of Justice Statistics. Grant*, (2009-DB), 2010.
- Bai, Lihui and Paul A Rubin. Combinatorial Benders Cuts for the Minimum Toll-booth Problem. *Operations Research*, 57(6):1510–1522, 2009. doi: 10.1287/opre.1090.0694. URL <http://or.journal.informs.org/cgi/content/abstract/opre.1090.0694v1>.
- Bardenet, Rémi, Odalric-Ambrym Maillard, and others. Concentration inequalities for sampling without replacement. *Bernoulli*, 21(3):1361–1385, 2015.
- Bobko, Philip, Philip L Roth, and Maury A Buster. The usefulness of unit weights in creating composite scores. A literature review, application to content validity, and meta-analysis. *Organizational Research Methods*, 10(4):689–709, 2007.
- Boyd, Stephen P and Lieven Vandenberghe. *Convex optimization*. Cambridge university press, 2004.
- Burgess, Ernest W. Factors determining success or failure on parole. *The workings of the indeterminate sentence law and the parole system in Illinois*, pages 221–234, 1928.
- Bussieck, Michael R and Stefan Vigerske. Minlp solver software. *Wiley Encyclopedia of Operations Research and Management Science*, 2010.
- Byrd, Richard H, Jorge Nocedal, and Richard A Waltz. Knitro: An integrated package for nonlinear optimization. In *Large-scale nonlinear optimization*, pages 35–59. Springer, 2006.
- Carrizosa, Emilio, Amaya Nogales-Gómez, and Dolores Romero Morales. Strongly agree or strongly disagree?: Rating features in support vector machines. *Information Sciences*, 329:256–273, 2016.
- Caruana, Rich and Alexandru Niculescu-Mizil. An empirical comparison of supervised learning algorithms. In *Proceedings of the 23rd international conference on Machine learning*, pages 161–168. ACM, 2006.
- Chevaleyre, Yann, Frédérick Koriche, and Jean-Daniel Zucker. Rounding methods for discrete linear classification. In *Proceedings of the 30th International Conference on Machine Learning (ICML-13)*, pages 651–659, 2013.

- Cranor, Lorrie Faith and Brian A LaMacchia. Spam! *Communications of the ACM*, 41(8): 74–83, 1998.
- DeGroot, Morris H and Stephen E Fienberg. The comparison and evaluation of forecasters. *The statistician*, pages 12–22, 1983.
- Duwe, Grant and KiDeuk Kim. Sacrificing accuracy for transparency in recidivism risk assessment: The impact of classification method on predictive performance. *Corrections*, pages 1–22, 2016.
- Ertekin, Şeyda and Cynthia Rudin. A bayesian approach to learning scoring systems. *Big Data*, 3(4):267–276, 2015.
- Franc, Vojtěch and Soeren Sonnenburg. Optimized cutting plane algorithm for support vector machines. In *Proceedings of the 25th international conference on Machine learning*, pages 320–327. ACM, 2008.
- Friedman, Jerome, Trevor Hastie, and Robert Tibshirani. Regularization paths for generalized linear models via coordinate descent. *Journal of Statistical Software*, 33(1):1–22, 2010.
- Gage, Brian F, Amy D Waterman, William Shannon, Michael Boehler, Michael W Rich, and Martha J Radford. Validation of clinical classification schemes for predicting stroke. *The Journal of the American Medical Association*, 285(22):2864–2870, 2001.
- Goel, Sharad, Justin M Rao, and Ravi Shroff. Precinct or prejudice? understanding racial disparities in new york city’s stop-and-frisk policy. *Understanding Racial Disparities in New York City’s Stop-and-Frisk Policy (March 2, 2015)*, 2015.
- Goffin, Jean-Louis and Jean-Philippe Vial. Convex nondifferentiable optimization: A survey focused on the analytic center cutting plane method. *Optimization Methods and Software*, 17(5):805–867, 2002.
- Goodman, Bryce and Seth Flaxman. Eu regulations on algorithmic decision-making and a” right to explanation”. *arXiv preprint arXiv:1606.08813*, 2016.
- Hastie, Trevor J., Robert John Tibshirani, and Jerome H Friedman. *The elements of statistical learning: data mining, inference, and prediction*. Springer, 2011.
- Hübner, Ruth and Anita Schöbel. When is rounding allowed in integer nonlinear optimization? *European Journal of Operational Research*, 237(2):404–410, 2014.
- Jennings, D, TM Amabile, and L Ross. Informal covariation assessment: Data-based vs. theory-based judgments. *Judgment under uncertainty: Heuristics and biases*, pages 211–230, 1982.
- Joachims, Thorsten, Thomas Finley, and Chun-Nam John Yu. Cutting-plane training of structural svms. *Machine Learning*, 77(1):27–59, 2009.
- Kelley, James E, Jr. The cutting-plane method for solving convex programs. *Journal of the Society for Industrial and Applied Mathematics*, 8(4):703–712, 1960.

- Knaus, William A, Jack E Zimmerman, Douglas P Wagner, Elizabeth A Draper, and Diane E Lawrence. APACHE-acute physiology and chronic health evaluation: a physiologically based classification system. *Critical Care Medicine*, 9(8):591–597, 1981.
- Knaus, William A, Elizabeth A Draper, Douglas P Wagner, and Jack E Zimmerman. APACHE II: a severity of disease classification system. *Critical Care Medicine*, 13(10): 818–829, 1985.
- Knaus, William A, DP Wagner, EA Draper, JE Zimmerman, Marilyn Bergner, PG Bastos, CA Sirio, DJ Murphy, T Lotring, and A Damiano. The APACHE III prognostic system. risk prediction of hospital mortality for critically ill hospitalized adults. *Chest Journal*, 100(6):1619–1636, 1991.
- Kodratoff, Y. The comprehensibility manifesto. *KDD Nugget Newsletter*, 94(9), 1994.
- Kohavi, Ron. Scaling up the accuracy of naive-bayes classifiers: A decision-tree hybrid. In *KDD*, pages 202–207, 1996.
- Latessa, Edward, Paula Smith, Richard Lemke, Matthew Makarios, and Christopher Lowenkamp. Creation and validation of the ohio risk assessment system: Final report. *Center for Criminal Justice Research, School of Criminal Justice, University of Cincinnati, Cincinnati, OH. Retrieved from http://www.ocjs.ohio.gov/ORAS_FinalReport.pdf*, 2009.
- Le Gall, Jean-Roger, Philippe Loirat, Annick Alperovitch, Paul Glaser, Claude Granthil, Daniel Mathieu, Philippe Mercier, Remi Thomas, and Daniel Villers. A simplified acute physiology score for icu patients. *Critical Care Medicine*, 12(11):975–977, 1984.
- Le Gall, Jean-Roger, Stanley Lemeshow, and Fabienne Saulnier. A new simplified acute physiology score (SAPS II) based on a european/north american multicenter study. *The Journal of the American Medical Association*, 270(24):2957–2963, 1993.
- Letham, Benjamin, Cynthia Rudin, Tyler H McCormick, and David Madigan. An interpretable stroke prediction model using rules and bayesian analysis. 2013.
- Levin, A Yu. On an algorithm for the minimization of convex functions. In *Soviet Mathematics Doklady*, volume 160, pages 1244–1247, 1965.
- Lichman, M. UCI machine learning repository, 2013. URL <http://archive.ics.uci.edu/ml>.
- Malioutov, Dmitry M and Kush R Varshney. Exact rule learning via boolean compressed sensing. In *ICML (3)*, pages 765–773, 2013.
- Mangasarian, Olvi L, W Nick Street, and William H Wolberg. Breast cancer diagnosis and prognosis via linear programming. *Operations Research*, 43(4):570–577, 1995.
- Miller, Alan J. Selection of subsets of regression variables. *Journal of the Royal Statistical Society. Series A (General)*, pages 389–425, 1984.

- Moreno, Rui P, Philipp GH Metnitz, Eduardo Almeida, Barbara Jordan, Peter Bauer, Ricardo Abizanda Campos, Gaetano Iapichino, David Edbrooke, Maurizia Capuzzo, and Jean-Roger Le Gall. SAPS 3 - from evaluation of the patient to evaluation of the intensive care unit. part 2: Development of a prognostic model for hospital mortality at icu admission. *Intensive Care Medicine*, 31(10):1345–1355, 2005.
- Moro, Sérgio, Paulo Cortez, and Paulo Rita. A data-driven approach to predict the success of bank telemarketing. *Decision Support Systems*, 62:22–31, 2014.
- Naoum-Sawaya, Joe and Samir Elhedhli. An interior-point Benders based branch-and-cut algorithm for mixed integer programs. *Annals of Operations Research*, 210(1):33–55, November 2010.
- Nguyen, Tan and Scott Sanner. Algorithms for direct 0-1 loss optimization in binary classification. In *ICML (3)*, pages 1085–1093, 2013.
- Pan, Sinno Jialin and Qiang Yang. A survey on transfer learning. *Knowledge and Data Engineering, IEEE Transactions on*, 22(10):1345–1359, 2010.
- Park, Jaehyun and Stephen Boyd. Concave quadratic cuts for mixed-integer quadratic problems. *arXiv preprint arXiv:1510.06421*, 2015a.
- Park, Jaehyun and Stephen Boyd. A semidefinite programming method for integer convex quadratic minimization. *arXiv preprint arXiv:1504.07672*, 2015b.
- Pennsylvania Commission on Sentencing, . Interim Report 4: Development of Risk Assessment Scale. Technical report, June 2012.
- R Core Team, . *R: A Language and Environment for Statistical Computing*. R Foundation for Statistical Computing, Vienna, Austria, 2014.
- Ridgeway, Greg. The pitfalls of prediction. *NIJ Journal*, National Institute of Justice, 271: 34–40, 2013.
- Schlimmer, Jeffrey Curtis. Concept acquisition through representational adjustment. 1987.
- Teo, Choon Hui, Alex Smola, SVN Vishwanathan, and Quoc Viet Le. A scalable modular convex solver for regularized risk minimization. In *Proceedings of the 13th ACM SIGKDD international conference on Knowledge discovery and data mining*, pages 727–736. ACM, 2007.
- Teo, Choon Hui, S Vishwanathan, Alex Smola, and Quoc V Le. Bundle methods for regularized risk minimization. *Journal of Machine Learning Research*, 1:55, 2009.
- U.S. Department of Justice, . The Mathematics of Risk Classification: Changing Data into Valid Instruments for Juvenile Courts. July 2005.
- U.S. Department of Justice, Bureau of Justice Statistics, . Recidivism of prisoners released in 1994. <http://doi.org/10.3886/ICPSR03355.v8>, 2014.

U.S. Sentencing Commission, . 2012 guidelines manual: Chapter four - criminal history and criminal livelihood, November 1987. URL <http://www.ussc.gov/guidelines-manual/2012/2012-4a11>.

Ustun, Berk and Cynthia Rudin. Supersparse linear integer models for optimized medical scoring systems. *Machine Learning*, pages 1–43, 2015. ISSN 0885-6125. doi: 10.1007/s10994-015-5528-6. URL <http://dx.doi.org/10.1007/s10994-015-5528-6>.

Zeng, Jiaming, Berk Ustun, and Cynthia Rudin. Interpretable classification models for recidivism prediction. *arXiv preprint arXiv:1503.07810*, 2015.

Appendix A. Proofs

A.1 Proof of Proposition 1

Proposition 1 (Bounds on Logistic Loss over a Bounded Coefficient Set)

Let $(\mathbf{x}_i, y_i)_{i=1}^N$ denote a training dataset where $\mathbf{x}_i \in \mathcal{X} \subset \mathbb{R}^d$ and $y_i \in \mathcal{Y} = \{-1, +1\}$ for all $i = 1, \dots, N$. Consider the value of the normalized logistic loss function for linear classifiers with coefficients $\boldsymbol{\lambda} \in \mathcal{L} \subset \mathbb{R}^d$:

$$l(\boldsymbol{\lambda}) = \frac{1}{N} \sum_{i=1}^N \log(1 + \exp(-\langle \boldsymbol{\lambda}, y_i \mathbf{x}_i \rangle))$$

If the coefficient set \mathcal{L} is bounded, then $l(\boldsymbol{\lambda}) \in [L^{\min}, L^{\max}]$ for all $\boldsymbol{\lambda} \in \mathcal{L}$ where:

$$\begin{aligned} L^{\min} &= \frac{1}{N} \sum_{i:y_i=+1} \log(1 + \exp(-s_i^{\max})) + \frac{1}{N} \sum_{i:y_i=-1} \log(1 + \exp(-s_i^{\min})), \\ L^{\max} &= \frac{1}{N} \sum_{i:y_i=+1} \log(1 + \exp(-s_i^{\min})) + \frac{1}{N} \sum_{i:y_i=-1} \log(1 + \exp(-s_i^{\max})), \end{aligned}$$

and,

$$\begin{aligned} s_i^{\min} &= \min_{\boldsymbol{\lambda} \in \mathcal{L}} \langle \boldsymbol{\lambda}, \mathbf{x}_i \rangle \quad \text{for } i = 1, \dots, N, \\ s_i^{\max} &= \max_{\boldsymbol{\lambda} \in \mathcal{L}} \langle \boldsymbol{\lambda}, \mathbf{x}_i \rangle \quad \text{for } i = 1, \dots, N. \end{aligned}$$

Proof Since the coefficient set \mathcal{L} is bounded, the data are $(\mathbf{x}_i, y_i)_{i=1}^N$ bounded, and the normalized logistic loss function $l(\boldsymbol{\lambda})$ is continuous, it follows that the value of $l(\boldsymbol{\lambda})$ is also bounded:

$$l(\boldsymbol{\lambda}) \in [\min_{\boldsymbol{\lambda} \in \mathcal{L}} l(\boldsymbol{\lambda}), \max_{\boldsymbol{\lambda} \in \mathcal{L}} l(\boldsymbol{\lambda})] \text{ for all } \boldsymbol{\lambda} \in \mathcal{L}.$$

Thus we only need to show that $L^{\min} \leq \min_{\boldsymbol{\lambda} \in \mathcal{L}} l(\boldsymbol{\lambda})$, and $L^{\max} \geq \max_{\boldsymbol{\lambda} \in \mathcal{L}} l(\boldsymbol{\lambda})$. For the lower bound, we observe that:

$$\begin{aligned} \min_{\boldsymbol{\lambda} \in \mathcal{L}} l(\boldsymbol{\lambda}) &= \min_{\boldsymbol{\lambda} \in \mathcal{L}} \frac{1}{N} \sum_{i=1}^N \log(1 + \exp(-\langle \boldsymbol{\lambda}, y_i \mathbf{x}_i \rangle)) \\ &\geq \frac{1}{N} \sum_{i=1}^N \min_{\boldsymbol{\lambda} \in \mathcal{L}} \log(1 + \exp(-\langle \boldsymbol{\lambda}, y_i \mathbf{x}_i \rangle)) \\ &= \frac{1}{N} \sum_{i=1}^N \log(1 + \exp(-\max_{\boldsymbol{\lambda} \in \mathcal{L}} \langle \boldsymbol{\lambda}, y_i \mathbf{x}_i \rangle)) \tag{15} \\ &= \frac{1}{N} \sum_{i:y_i=+1} \log(1 + \exp(-\max_{\boldsymbol{\lambda} \in \mathcal{L}} \langle \boldsymbol{\lambda}, \mathbf{x}_i \rangle)) + \frac{1}{N} \sum_{i:y_i=-1} \log(1 + \exp(-\min_{\boldsymbol{\lambda} \in \mathcal{L}} \langle \boldsymbol{\lambda}, \mathbf{x}_i \rangle)) \\ &= \frac{1}{N} \sum_{i:y_i=+1} \log(1 + \exp(-s_i^{\min})) + \frac{1}{N} \sum_{i:y_i=-1} \log(1 + \exp(-s_i^{\max})) \\ &= L^{\min}. \end{aligned}$$

Here (15) follows from the fact that the logistic loss function is monotonically decreasing in $-\langle \boldsymbol{\lambda}, y_i \mathbf{x}_i \rangle$.

Similarly, for the upper bound, we observe that:

$$\begin{aligned}
 \max_{\boldsymbol{\lambda} \in \mathcal{L}} l(\boldsymbol{\lambda}) &= \max_{\boldsymbol{\lambda} \in \mathcal{L}} \frac{1}{N} \sum_{i=1}^N \log(1 + \exp(-\langle \boldsymbol{\lambda}, y_i \mathbf{x}_i \rangle)) \\
 &\leq \frac{1}{N} \sum_{i=1}^N \max_{\boldsymbol{\lambda} \in \mathcal{L}} \log(1 + \exp(-\langle \boldsymbol{\lambda}, y_i \mathbf{x}_i \rangle)) \\
 &= \frac{1}{N} \sum_{i=1}^N \log(1 + \exp(-\min_{\boldsymbol{\lambda} \in \mathcal{L}} \langle \boldsymbol{\lambda}, y_i \mathbf{x}_i \rangle)) \\
 &= \frac{1}{N} \sum_{i: y_i = +1} \log(1 + \exp(-\min_{\boldsymbol{\lambda} \in \mathcal{L}} \langle \boldsymbol{\lambda}, \mathbf{x}_i \rangle)) + \frac{1}{N} \sum_{i: y_i = -1} \log(1 + \exp(-\max_{\boldsymbol{\lambda} \in \mathcal{L}} \langle \boldsymbol{\lambda}, \mathbf{x}_i \rangle)) \\
 &= \frac{1}{N} \sum_{i: y_i = +1} \log(1 + \exp(-s_i^{\min})) + \frac{1}{N} \sum_{i: y_i = -1} \log(1 + \exp(-s_i^{\max})) \\
 &= L^{\max}.
 \end{aligned} \tag{16}$$

■

A.2 Proof of Proposition 2

Proposition 2 (Upper Bound on Optimal Number of Non-Zero Coefficients)

Given an upper bound on the objective value $V^{\max} \geq V(\boldsymbol{\lambda}^*)$, and a lower bound on the loss function $L^{\min} \leq l(\boldsymbol{\lambda}^*)$, we can derive an upper bound on the value of the number of optimal non-zero coefficients $R^{\max} \geq \|\boldsymbol{\lambda}^*\|_0$ as

$$R^{\max} = \left\lfloor \frac{V^{\max} - L^{\min}}{C_0} \right\rfloor$$

Proof We are given that $V^{\max} \geq V(\boldsymbol{\lambda}^*)$ where $V(\boldsymbol{\lambda}^*) := l(\boldsymbol{\lambda}^*) + C_0 \|\boldsymbol{\lambda}^*\|_0$ by definition. Thus, we can recover the upper bound from Proposition 2 as follows:

$$\begin{aligned}
 l(\boldsymbol{\lambda}^*) + C_0 \|\boldsymbol{\lambda}^*\|_0 &\leq V^{\max}, \\
 \|\boldsymbol{\lambda}^*\|_0 &\leq \frac{V^{\max} - l(\boldsymbol{\lambda}^*)}{C_0}, \\
 \|\boldsymbol{\lambda}^*\|_0 &\leq \frac{V^{\max} - L^{\min}}{C_0},
 \end{aligned} \tag{17}$$

$$\|\boldsymbol{\lambda}^*\|_0 \leq \left\lfloor \frac{V^{\max} - L^{\min}}{C_0} \right\rfloor. \tag{18}$$

Here, (17) follows from the fact that $L^{\min} \leq l(\boldsymbol{\lambda}^*)$ by definition, and (18) follows from the fact that the number of non-zero coefficients is a natural number. ■

A.3 Proof of Proposition 3

Proposition 3 (Upper Bound on Optimal Loss)

Given an upper bound on the objective value $V^{\max} \geq V(\boldsymbol{\lambda}^*)$, and a lower bound on the number of non-zero coefficients $R^{\min} \leq \|\boldsymbol{\lambda}^*\|_0$, we can derive an upper bound on value of the loss function $L^{\max} \geq l(\boldsymbol{\lambda}^*)$ where

$$L^{\max} = V^{\max} - C_0 R^{\min}.$$

Proof We are given that $V^{\max} \geq V(\boldsymbol{\lambda}^*)$ where $V(\boldsymbol{\lambda}^*) := l(\boldsymbol{\lambda}^*) + C_0 \|\boldsymbol{\lambda}^*\|_0$ by definition. Thus, we can recover the upper bound from Proposition 3 as follows:

$$\begin{aligned} l(\boldsymbol{\lambda}^*) + C_0 \|\boldsymbol{\lambda}^*\|_0 &\leq V^{\max}, \\ l(\boldsymbol{\lambda}^*) &\leq V^{\max} - C_0 \|\boldsymbol{\lambda}^*\|_0, \\ l(\boldsymbol{\lambda}^*) &\leq V^{\max} - C_0 R^{\min}. \end{aligned}$$

Here, the last line follows from the fact that $R^{\min} \leq \|\boldsymbol{\lambda}^*\|_0$ by definition. ■

A.4 Proof of Proposition 4

Proposition 4 (Lower Bound on Optimal Loss)

Given a lower bound on the objective value $V^{\min} \leq V(\boldsymbol{\lambda}^*)$, and an upper bound on the number of non-zero coefficients $R^{\max} \geq \|\boldsymbol{\lambda}^*\|_0$, we can derive a lower bound on value of the loss function $L^{\min} \leq l(\boldsymbol{\lambda}^*)$ where

$$L^{\min} = V^{\min} - C_0 R^{\max}.$$

Proof We are given that $V^{\min} \leq V(\boldsymbol{\lambda}^*)$ where $V(\boldsymbol{\lambda}^*) := l(\boldsymbol{\lambda}^*) + C_0 \|\boldsymbol{\lambda}^*\|_0$ by definition. Thus, we can recover the lower bound from Proposition 4 as follows:

$$\begin{aligned} l(\boldsymbol{\lambda}^*) + C_0 \|\boldsymbol{\lambda}^*\|_0 &\geq V^{\min}, \\ l(\boldsymbol{\lambda}^*) &\geq V^{\min} - C_0 \|\boldsymbol{\lambda}^*\|_0, \\ l(\boldsymbol{\lambda}^*) &\geq V^{\min} - C_0 R^{\max}. \end{aligned}$$

Here, the last line follows from the fact that $R^{\max} \geq \|\boldsymbol{\lambda}^*\|_0$ by definition. ■

A.5 Proof of Theorem 1

Theorem 1 (Generalization of Sampled Loss on Finite Coefficient Set)

Let $\mathcal{D}_N = (\mathbf{x}_i, y_i)_{i=1}^N$ denote a finite training set composed of $N > 1$ points and $\mathcal{D}_M = (\mathbf{x}_i, y_i)_{i=1}^M$ denote a sample of M points drawn without replacement from \mathcal{D}_N . Let $\boldsymbol{\lambda}$ denote the coefficients of a linear classifier from a finite set \mathcal{L} . Then, for all $\varepsilon > 0$, we have that

$$\Pr \left(\max_{\boldsymbol{\lambda} \in \mathcal{L}} \left(l_N(\boldsymbol{\lambda}) - l_M(\boldsymbol{\lambda}) \right) \geq \varepsilon \right) \leq |\mathcal{L}| \exp \left(- \frac{2\varepsilon^2}{\left(\frac{1}{M}\right)\left(1 - \frac{M}{N}\right)\left(1 + \frac{M}{N}\right)\Delta^{\max}(\mathcal{L}, \mathcal{D}_N)^2} \right)$$

where

$$\Delta^{\max}(\mathcal{L}, \mathcal{D}_N) = \max_{\boldsymbol{\lambda} \in \mathcal{L}} \left(\max_{i=1, \dots, N} l_i(\boldsymbol{\lambda}) - \min_{i=1, \dots, N} l_i(\boldsymbol{\lambda}) \right).$$

Proof For a fixed set coefficients $\boldsymbol{\lambda} \in \mathcal{L}$, consider a finite sample of N points composed of the values for the loss function $l_i(\boldsymbol{\lambda})$ for each example in the full training dataset $\mathcal{D}_N = (\mathbf{x}_i, y_i)_{i=1}^N$. Let $l_N(\boldsymbol{\lambda}) = \frac{1}{N} \sum_{i=1}^N l_i(\boldsymbol{\lambda})$ and $l_M(\boldsymbol{\lambda}) = \frac{1}{M} \sum_{i=1}^M l_i(\boldsymbol{\lambda})$. Then, the Hoeffding-Serfling inequality (see e.g., Theorem 2.4 in Bardenet et al., 2015) guarantees the following for all $\varepsilon > 0$:

$$\Pr (l_N(\boldsymbol{\lambda}) - l_M(\boldsymbol{\lambda}) \geq \varepsilon) \leq \exp \left(- \frac{2\varepsilon^2}{\left(\frac{1}{M}\right)\left(1 - \frac{M}{N}\right)\left(1 + \frac{M}{N}\right)\Delta(\boldsymbol{\lambda}, \mathcal{D}_N)^2} \right)$$

where

$$\Delta(\boldsymbol{\lambda}, \mathcal{D}_N) = \max_{i=1, \dots, N} l_i(\boldsymbol{\lambda}) - \min_{i=1, \dots, N} l_i(\boldsymbol{\lambda}).$$

We recover the desired inequality by generalizing this bound to hold for all $\boldsymbol{\lambda} \in \mathcal{L}$ as follows.

$$\begin{aligned} \Pr \left(\max_{\boldsymbol{\lambda} \in \mathcal{L}} \left(l_N(\boldsymbol{\lambda}) - l_M(\boldsymbol{\lambda}) \right) \geq \varepsilon \right) &= \Pr \left(\bigcup_{\boldsymbol{\lambda} \in \mathcal{L}} \left(l_N(\boldsymbol{\lambda}) - l_M(\boldsymbol{\lambda}) \geq \varepsilon \right) \right), \\ &\leq \sum_{\boldsymbol{\lambda} \in \mathcal{L}} \Pr (l_N(\boldsymbol{\lambda}) - l_M(\boldsymbol{\lambda}) \geq \varepsilon), \end{aligned} \quad (19)$$

$$\leq \sum_{\boldsymbol{\lambda} \in \mathcal{L}} \exp \left(- \frac{2\varepsilon^2}{\left(\frac{1}{M}\right)\left(1 - \frac{M}{N}\right)\left(1 + \frac{M}{N}\right)\Delta(\boldsymbol{\lambda}, \mathcal{D}_N)^2} \right), \quad (20)$$

$$\leq |\mathcal{L}| \exp \left(- \frac{2\varepsilon^2}{\left(\frac{1}{M}\right)\left(1 - \frac{M}{N}\right)\left(1 + \frac{M}{N}\right)\Delta^{\max}(\mathcal{L}, \mathcal{D}_N)^2} \right). \quad (21)$$

Here, (19) follows from the union bound, (20) follows from the Hoeffding Serfling inequality, (21) follows from the fact that $\Delta(\boldsymbol{\lambda}, \mathcal{D}_N) \leq \Delta^{\max}(\mathcal{L}, \mathcal{D}_N)$ given that $\boldsymbol{\lambda} \in \mathcal{L}$. \blacksquare

A.6 Proof of Corollary 1

Corollary 1 (Update Probabilities of Rounding Heuristics on Sampled Data)

Consider a rounding heuristic that takes as input a vector of continuous coefficients $\boldsymbol{\rho} = (\rho_1, \dots, \rho_d) \in \text{conv}(\mathcal{L})$ and produces as output a vector of integer coefficients $\boldsymbol{\lambda} \in \mathcal{L}(\boldsymbol{\rho})$ where

$$\mathcal{L}(\boldsymbol{\rho}) = \left(\boldsymbol{\lambda} \in \mathcal{L} \mid \lambda_j \in \{ \lceil \rho_j \rceil, \lfloor \rho_j \rfloor \} \text{ for } j = 1, \dots, d \right)$$

Consider evaluating the rounding heuristic using a sample of M points $\mathcal{D}_M = (\mathbf{x}_i, y_i)_{i=1}^M$ drawn without replacement from the full training dataset $\mathcal{D}_N = (\mathbf{x}_i, y_i)_{i=1}^N$. Pick a tolerance $\delta > 0$. Given rounded coefficients $\boldsymbol{\lambda} \in \mathcal{L}(\boldsymbol{\rho})$, compute $V_M(\boldsymbol{\lambda})$. If

$$V_M(\boldsymbol{\lambda}) < V^{\max} - \varepsilon_\delta,$$

then w.p. at least $1 - \delta$, we have

$$V_N(\boldsymbol{\lambda}) \leq V^{\max}$$

Proof We will first show that for any tolerance that we pick $\delta > 0$, the prescribed choice of ε_δ will ensure that $V_N(\boldsymbol{\lambda}) - V_M(\boldsymbol{\lambda}) \leq \varepsilon_\delta$ w.p. at least $1 - \delta$. Restating the result of Theorem 1, we have that for any $\varepsilon > 0$:

$$\Pr \left(\max_{\boldsymbol{\lambda} \in \mathcal{L}} \left(l_N(\boldsymbol{\lambda}) - l_M(\boldsymbol{\lambda}) \right) \geq \varepsilon \right) \leq |\mathcal{L}| \exp \left(- \frac{2\varepsilon^2}{\left(\frac{1}{M}\right)\left(1 - \frac{M}{N}\right)\left(1 + \frac{M}{N}\right)\Delta^{\max}(\mathcal{L}, \mathcal{D}_N)^2} \right). \quad (22)$$

Note that $l_N(\boldsymbol{\lambda}) - l_M(\boldsymbol{\lambda}) = V_N(\boldsymbol{\lambda}) - V_M(\boldsymbol{\lambda})$ for any fixed $\boldsymbol{\lambda}$. In addition, note that the set of rounded coefficients $\mathcal{L}(\boldsymbol{\rho})$ contains at most $|\mathcal{L}(\boldsymbol{\rho})| \leq 2^d$ coefficients vectors. Therefore, in this setting, (22) implies that for any $\varepsilon > 0$,

$$\Pr(V_N(\boldsymbol{\lambda}) - V_M(\boldsymbol{\lambda}) \geq \varepsilon) \leq 2^d \exp \left(- \frac{2\varepsilon^2}{\left(\frac{1}{M}\right)\left(1 - \frac{M}{N}\right)\left(1 + \frac{M}{N}\right)\Delta(\mathcal{L}(\boldsymbol{\rho}), \mathcal{D}_N)^2} \right). \quad (23)$$

By setting $\varepsilon = \varepsilon_\delta$ and simplifying the terms on the right hand side in (23), we can see that

$$\Pr(V_N(\boldsymbol{\lambda}) - V_M(\boldsymbol{\lambda}) \geq \varepsilon_\delta) \leq \delta.$$

Thus, the prescribed value of ε_δ ensures that $V_N(\boldsymbol{\lambda}) - V_M(\boldsymbol{\lambda}) \leq \varepsilon_\delta$ w.p. at least $1 - \delta$.

Since we have set ε_δ so that $V_N(\boldsymbol{\lambda}) - V_M(\boldsymbol{\lambda}) \leq \varepsilon_\delta$ w.p. at least $1 - \delta$, we now only need to show any $\boldsymbol{\lambda}$ that satisfies $V_M(\boldsymbol{\lambda}) < V^{\max} - \varepsilon_\delta$ will also satisfy $V_N(\boldsymbol{\lambda}) \leq V^{\max}$ to complete the proof. To see this, observe that:

$$\begin{aligned} V_N(\boldsymbol{\lambda}) - V_M(\boldsymbol{\lambda}) &\leq \varepsilon_\delta, \\ V_N(\boldsymbol{\lambda}) &\leq V_M(\boldsymbol{\lambda}) + \varepsilon_\delta, \\ V_N(\boldsymbol{\lambda}) &< V^{\max}. \end{aligned} \quad (24)$$

Here, (24) follows from the fact that $V_M(\boldsymbol{\lambda}) < V^{\max} - \varepsilon_\delta \implies V_M(\boldsymbol{\lambda}) + \varepsilon_\delta < V^{\max}$ \blacksquare

Appendix B. Details on Experimental Comparison with Simulated Data

B.1 Data Simulation Procedure

We simulated data from the `breastcancer` dataset (Mangasarian et al., 1995). The original dataset can be obtained from the UCI ML repository (Lichman, 2013), and has a total of $N = 683$ samples and $d = 9$ features $x_{ij} \in \{0, \dots, 10\}$. Using the original dataset, we generated a collection of simulated datasets using the procedure outlined in Algorithm 7. Specifically, we first simulated the largest dataset we needed (with $N^{\max} = 10^6$ samples and $d^{\max} = 30$ features) by replicating features and samples from the original dataset and adding a small amount of normally distributed noise. Next, we created smaller datasets by taking *nested* subsets of the samples and the features. This ensured that any simulated dataset with d features and N samples contains all of the features and examples for a simulated dataset with $d' < d$ features and $N' < N$ samples. We designed this procedure to have the following special properties:

- It would produce difficult instances of the risk score problem. Here, RISKSLIMMINLP instances for simulated datasets with $d > 9$ are challenging in terms of feature selection because they contain replicates of the original 9 features, which are strongly correlated with each another. Feature selection becomes exponentially harder when collections of highly correlated features are used, since this means that there are an exponentially larger number of slightly suboptimal solutions.
- We could make inferences about the optimal objective value of RISKSLIMMINLP instances we may not have been able to solve. Say, for example, that we could not solve an instance of the risk score problem for the simulated dataset with $(d, N) = (20, 10^6)$, but could solve an instance for the simulated dataset with $(d, N) = (10, 10^6)$. In this case, we knew that the optimal objective value of the $(d, N) = (20, 10^6)$ instance had to be less than or equal to the optimal objective value of the $(d, N) = (10, 10^6)$ instance because the $(d, N) = (20, 10^6)$ dataset contained all of the features as the $(d, N) = (10, 10^6)$ dataset.

B.2 Implementation Details

We trained risk scores for all simulated datasets by solving RISKSLIMMINLP using the following techniques: (i) conventional CP (Algorithm 1); (ii) and the lattice CP algorithm (Algorithm 2); (iii) an active set MINLP algorithm; (iv) an interior direct MINLP algorithm; (v) an interior CG MINLP algorithm.

We solved all instances on a 3.33 GHz Intel Xeon CPU with 16GB of RAM and enforced a hard limit on training time at 6 hours. If an algorithms did not converge to optimality in 6 hours, we reported results based on the best feasible solution that was produced. We implemented both cutting plane techniques using the CPLEX 12.6.3 API, which we accessed using Python. We solved instances using MINLP algorithms using the Artelsys Knitro 9.0 MINLP solver (Byrd et al., 2006), which we accessed through MATLAB 2015b.

Algorithm 7 Simulation Procedure

Input

$X^{\text{original}} = [x_{ij}]_{i=1\dots N^{\text{original}}, j=1\dots d^{\text{original}}}$, feature matrix of original dataset
 $Y^{\text{original}} = [y_i]_{i=1\dots N^{\text{original}}}$, label matrix of original dataset
 $d^1 \dots d^{\text{max}}$ s.t. $0 < d^1 < \dots < d^{\text{max}}$, desired dimensions for simulated datasets
 $N^1 \dots N^{\text{max}}$ s.t. $0 < N^1 < \dots < N^{\text{max}}$, desired sample sizes for simulated datasets

Initialize

$\mathcal{J}^{\text{original}} = [1, \dots, d^{\text{original}}]$, index array for original features
 $\mathcal{J}^{\text{max}} \leftarrow []$, index array of features for largest simulated dataset
 $m^{\text{full}} \leftarrow \lfloor d^{\text{max}}/d^{\text{original}} \rfloor$
 $m^{\text{remainder}} \leftarrow d^{\text{max}} - d^{\text{original}}$

STEP 1: Generate Largest Dataset

```

1 for  $m = 1, \dots, m^{\text{full}}$  do
2    $\mathcal{J}^{\text{max}} \leftarrow [\mathcal{J}^{\text{max}}, \text{RANDOMPERMUTE}(\mathcal{J}^{\text{original}})]$ 
3 end for
4    $\mathcal{J}^{\text{max}} \leftarrow [\mathcal{J}^{\text{max}}, \text{RANDOMSAMPLEWITHOUTREPLACEMENT}(\mathcal{J}^{\text{original}}, m^{\text{remainder}})]$ 

4 for  $i = 1, \dots, N^{\text{max}}$  do
5   sample  $l$  with replacement from  $1, \dots, N^{\text{original}}$ 
6    $y_i^{\text{max}} \leftarrow y_l$ 
7   for  $j = 1, \dots, d^{\text{max}}$  do
8      $k \leftarrow \mathcal{J}^{\text{max}}[j]$ 
9     sample  $\varepsilon$  from  $\text{Normal}(0, 0.5)$ 
10     $x_{ij}^{\text{max}} \leftarrow \lceil x_{l,k} + \varepsilon \rceil$   $\triangleright$  create discrete features that are noisy versions of original features
11     $x_{ij}^{\text{max}} \leftarrow \min(10, \max(0, x_{ij}^{\text{max}}))$   $\triangleright$  ensure that new features are within bounds of old features
12  end for
13 end for
14  $X^{\text{max}} \leftarrow [x_{ij}]_{i=1\dots N^{\text{max}}, j=1\dots d^{\text{max}}}$ 
15  $Y^{\text{max}} \leftarrow [y_i^{\text{max}}]_{i=1\dots N^{\text{max}}}$ 
    
```

STEP 2: Generate Smaller Datasets

```

16 for  $d = [d^1, \dots, d^{\text{max}}]$  do
17   for  $N = [N^1, \dots, N^{\text{max}}]$  do
18      $X^{(N,d)} = X^{\text{max}}[1 : N, 1 : d]$ 
19      $Y^N = Y^{\text{max}}[1 : N]$ 
20   end for
21 end for
    
```

Output: simulated datasets $(X^{(N,d)}, Y^N)$ for all $N^1 \dots N^{\text{max}}$ and $d^1 \dots d^{\text{max}}$.

B.3 Results for All MINLP Algorithms

We examined the performance of 3 MINLP algorithms in Artelsys Knitro 9.0, namely: an active set algorithm (MINLP Active Set); an interior-point algorithm (MINLP Interior); an interior-point algorithm where the primal-dual KKT system is solved with a conjugate gradient method (MINLP Interior CG). We only show results from MINLP Active Set in Figure 15 because all three algorithms behave similarly. For completeness, we include the same plots for the remaining MINLP algorithms in Figure 15.

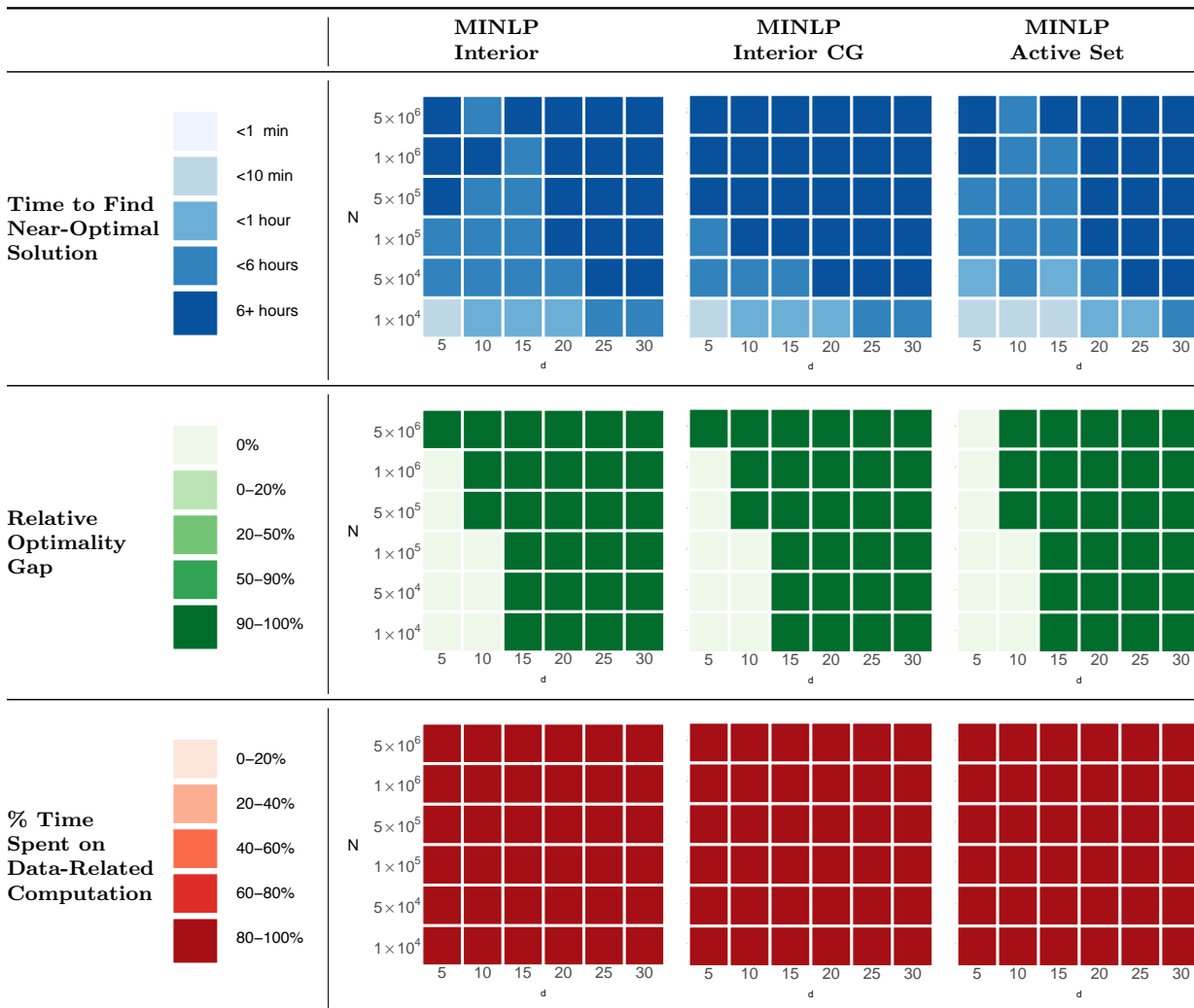


Figure 15: Performance of MINLP algorithms to solve RISKSLIMMINLP on simulated datasets with varying dimensions d and sample sizes N . All MINLP algorithms exhibit similar performance in terms of the metrics that we consider in Figure .